The inherent multidimensionality of temporal variability:

How common and rare species shape stability patterns

Jean-François Arnoldi[1,2,*], Michel Loreau[1], and Bart Haegeman[1]

[2] *Centre for Biodiversity Theory and Modelling, Theoretical and Experimental Ecology Station,*

CNRS and Paul Sabatier University, 09200 Moulis, France.

[2] *Zoology department, School of Natural Sciences, Trinity College Dublin, Ireland.*

[*]arnoldij@tcd.ie

1

Abstract

Empirical knowledge of ecosystem stability and ~~of~~ diversity-stability relationships is mostly ~~built~~ based on the analysis of temporal variability of population and ecosystem properties. Variability, however, often depends on external factors that act as disturbances, making it difficult to compare its value across systems ~~,~~ and relate it to other stability concepts. Here we show how variability, when ~~seen~~ viewed as a response to stochastic perturbations ~~of various types~~, can reveal inherent stability properties of ecological communities, with clear connections with other stability ~~measures~~ notions. This requires abandoning one-dimensional representations ~~of stability~~, in which a single variability measurement is taken as a proxy for how stable a system is, and instead consider the whole ~~variability spectrum, i.e. the distribution of the system's response to the vast~~ set of variability values associated to a given community, reflecting the whole set of perturbations that can generate variability. ~~In species-rich model communities~~ Against the vertiginous dimensionality of the perturbation set, we show that ~~there exist generic patterns for which specific abundance classes of species govern variability. In particular~~ a generic variability-abundance pattern emerges from community assembly, which relates variability to the abundance of perturbed species. As a consequence, the response to stochastic immigration is ~~typically~~ governed by rare species while common species drive the response to environmental perturbations. ~~We show that~~ In particular, the contrasting contributions of different species abundance classes can ~~be responsible for~~ lead to opposite diversity-stability patterns ~~. More generally, our work proposes~~, which can be understood from basic statistics of the abundance distribution. Our work shows that a multidimensional perspective on ~~stability~~ variability allows one to better appreciate the dynamical richness of ~~ecosystems, and to better understand the causes and consequences~~ ecological systems and the underlying meaning of their stability patterns.

Introduction

Ecological stability is a notoriously elusive and multifaceted concept (Pimm, 1984; Donohue et al., 2016). At the same time, understanding its drivers and relationship with biodiversity is a fundamental, pressing, yet enduring challenge for ecology (Elton, 1946; MacArthur, 1955; May, 1973a; McCann, 2000). ~~Temporal variability (with lower variability being interpreted as a higher stability)~~ The temporal variability of populations or ecosystem functions, where lower variability is interpreted as higher stability, is an attractive facet of ecological stability, for several ~~notable~~ reasons. First, variability is empirically accessible using simple time-series statistics ~~such as variance and coefficient of variation (Tilman et al., 1996; Yachi and Loreau, 1999)~~ ~~.~~ (Tilman et al., 1996). Second, variability – or its inverse, invariability – is a flexible notion that can be applied across levels of biological organization (Haegeman et al., 2016) and spatial scales (Wang and Loreau, 2014; Wang et al., 2017). Third, variability ~~is~~ can be indicative of the risk that an ecological system might go extinct, collapse or experience a regime shift (Scheffer et al., 2009). During the last decade, the relationship between biodiversity and ecological stability has thus been extensively studied empirically ~~by focusing on the temporal variability of populations or ecosystem properties (Tilman et al., 2006; Jiang and Pu, 2009; Hector et al., 2010; Campb~~ using invariability as a measure of stability (Tilman et al., 2006; Jiang and Pu, 2009; Hector et al., 2010; C .

In ~~the~~ a literal sense, stability is the property of what tends to remain unchanged (Pimm, 1991). Variability denotes the tendency of a variable to change in time, so that its inverse, invariability, fits this intuitive definition ~~of stability~~. However, variability is not necessarily an inherent property of the system that is observed (e.g., a community of interacting species), as it typically also depends on external factors that act as perturbations, and generate the observed variability. In other words, the variability of ~~an ecological~~ a community is not a prop-

4

erty of that community *alone.* It may be caused by a particular perturbation regime ~~(e.g. temperature fluctuations), and a different perturbation regime (e.g. precipitation fluctuations) would~~ so that a different regime could lead to a different value of variability. Stronger perturbations will generate larger fluctuations, and the way a perturbation's intensity is distributed and correlated across species is also critical. In other words, a variability measurement reflects the response of a system to the specific environmental context in which it is embedded.

~~That being said~~Despite this complexity, quantifying the fluctuations of ~~,~~ an ecosystem property (e.g., primary production~~of an ecosystem~~) can be of foremost practical interest ~~,~~ as it provides ~~—~~a measure of predictability in a given environmental context ~~— a measure of its predictability~~ (Griffin et al., 2009). However, to generalize results beyond the specific context in which variability is measured, use variability to compare the stability of different systems, establish links between different stability notions, or reconcile the conflicting diversity-stability patterns and predictions reported in the empirical and theoretical literature (Ives and Carpenter, 2007), one needs to know how variability measurements can reflect a system's inherent dynamical ~~properties~~features.

~~To do so~~Here, we adopt an approach in which stability is viewed as the inherent ability of a dynamical system to endure perturbations (Fig. 1A). ~~As a consequence,~~ For simplicity we will restrict to systems near equilibrium, by opposition to, e.g., limit cycles or chaotic attractors. We propose that a measure of stability should ~~not be associated with~~ reflect, not a particular perturbation (as in Fig. 1B), but ~~instead should reflect~~ a system's propensity to withstand ~~perturbations *in general.*~~

~~We~~ *a whole class* of perturbations. We therefore consider a vast ~~range of possible perturbations that can generate variability~~perturbation set, and study ~~, instead of a unique measure,~~ ~~the corresponding broad~~ the corresponding range of community responses ~~, which we call *variability spectrum*~~ (Fig. 1C). Even from a theoretical perspective, considering all possi-

5

A System-view on stability

perturbation ⟶ system ⟶ response

B Variability dependent on system and perturbation

perturbation ⟶ system ⟶ single variability value

C Variability as an inherent system property

perturbation 1
perturbation 2
perturbation 3 ⟶ system ⟶ variability distribution
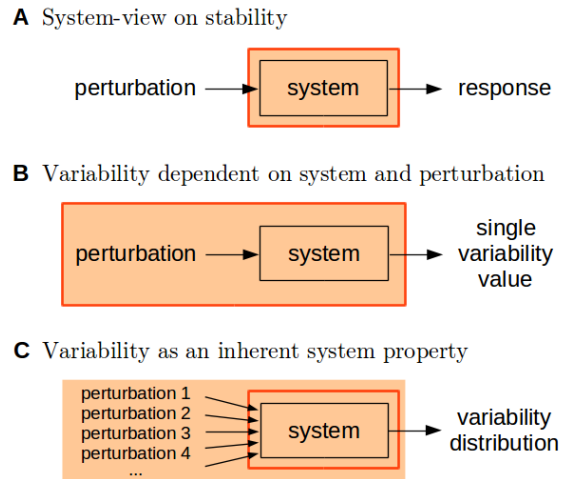perturbation 4
...

Figure 1: Variability vs stability. A: Stability quantifies the way a system responds to perturbations, seen as an inherent property of the system (indicated by the red framed box). B: By contrast, temporal variability is typically a feature of both the system studied and external factors that act as perturbations. C: For variability to ~~measure the stability~~ be an inherent property of the system, one can consider a whole set of perturbations, thus integrating out the dependence on specific external factors.~~Here we analyze the patterns that emerge from this approach.~~

ble perturbations that an ecosystem can face is a daunting task. We will thus restrict our attention to model ecological communities near equilibrium, perturbed by weak stochastic perturbations, and derive analytical formulas for two complementary features of the set of their variability values: its average and maximum, corresponding to the mean- and worst-case perturbation scenarios, respectively.

After having developed a general theory of variability that can be applied to any model community near equilibrium, we turn our attention to species-rich communities that are assembled from nonlinear dynamics. We show that a generic variability-abundance pattern can emerge from the complex interactions between species during assembly. We argue that this pattern, in conjunction with the type of perturbations considered (environmental, demographic, or caused by stochastic immigration), determines the specific species abundance class that governs the variability distribution. In particular, we establish a generic link between rare species, worst-case variability, and asymptotic resilience – the long-term rate of return to equilibrium following a pulse perturbation. We finally illustrate that the contrasting contributions of various species abundance classes can be responsible for opposite diversity-invariability patterns.

The goal of our work is (i) to demonstrate that variability is an inherently multidimensional notion, reflecting the multidimensionality of an ecosystem's responses to perturbations; (ii) to show that clear patterns exist in ecosystem responses to per-

7

turbations~~reflecting~~, which reflect the dynamical properties of distinct species abundance classes; (iii) to argue that, in order to compare and predict ~~stability~~ variability patterns, it is paramount to first identify to which abundance class these patterns or predictions refer to; and finally, (iv) to propose that a multidimensional perspective on ~~stability~~ variability allows one to better appreciate the dynamical richness of ecosystems, and the underlying meaning of their stability patterns.

Conceptual framework

~~To make the schematic representation of Fig. 1 more concrete, we will restrict to the mathematically convenient setting of communities modeled~~ We focus on communities modelled as dynamical systems ~~close to an~~ at equilibrium, and study their responses to a whole class of stochastic white-noise forcing. In this section we outline the theory, focusing on ecological intuitions, while Appendix A through D provides a self-contained presentation of its mathematical foundations. Our work follows traditional approaches of theoretical ecology (May, 1973a; Ives et al., 2003), extending the analysis to encompass a large perturbation set.

Perturbed communities

~~Consider a community of S interacting species whose biomass are modeled as continuous interacting dynamical variables~~

Let $N_i(t)$ ~~approaching an equilibrium value $N_i > 0$, with $i = 1, 2, ...S$. Let $x_i(t) = N_i(t) - N_i$ denote the difference between~~ represent the abundance (or biomass) of species i ~~'s biomass $N_i(t)$~~ at time t, and ~~its~~ $x_i(t) = N_i(t) - N_i$ its displacement from an equilibrium value N_i, with i running over S coexisting species that form an ecological community. We model ~~biomass fluctuations~~ fluctuations in abundance (hence variability) as a response to ~~weak~~ some stochas-

8

tic forcing. We focus on stationary fluctuations caused by weak perturbations with zero mean[1], which are governed by the following dynamical system, written from the perspective of species i as

$$\frac{d}{dt}\underbrace{x_i(t)}_{\text{fluctuations}} = \sum_{j=1}^{S}\underbrace{A_{ij}x_j(t)}_{\text{interactions}} + \underbrace{\sigma_i\sqrt{N_i}^{\alpha}\,\xi_i(t)}_{\text{perturbation}}. \tag{1}$$

In this expression, the coefficients A_{ij} represent the effect that a small change of abundance of species j has on the abundance of species i. Organized in the *community matrix* $A = (A_{ij})$, they encode the linearization of the nonlinear system of which (N_i) is an equilibrium. In the perturbation term,

$$\sigma_i N_i^{\frac{\alpha}{2}}\,W_i(t),$$

$\xi_i(t)$ denotes a standard white-noise source (Arnold, 1974; Van Kampen, 1997). In discrete time $\xi_i(t)$ would be a normally distributed random variable with zero mean and unit variance, drawn independently at each time step (Appendix A).

Community models of the form eq. (1) were studied by Ives et al. (2003) to analyze ecological time series. In their approach, stability properties are inferred from the system's response to specific perturbations. Here we build on a similar formalism, but explicitly explore a

---

[1] If the perturbation effect does not have zero mean, an equivalent system can be studied by redefining the equilibrium as the mean of species time series.

vast set of possible perturbations. Although environmental often follow temporal patterns ~~(Vasseur and Yodzis, 2004; Ruokolainen and Fowler, 2008), the absence of temporal autocorrelation~~ ~~is not a critical assumption for what follows. We will allow~~ (Vasseur and Yodzis, 2004; Ruokolainen et al., 2 we will not consider autocorrelated perturbations. It would thus be interesting to extend the analysis to more general temporal structures of perturbations, as well as to nonlinear behaviors. What we will explicitly consider, however, ~~for~~ are temporal correlations between ~~$W_i(t)$ and $W_j(t)$, which could model~~ $\xi_i(t)$ and $\xi_j(t)$, a situation in which individuals of species i and j are similar in their perception of a given perturbation. ~~The perturbation term (??), representing the direct effect that a perturbation has on the biomass of species i, is written as some power of N_i, and is proportional to a species-specific term $\sigma_i W_i(t)$. The latter is a function of the perturbation itself, and of traits of species i which determine how individuals of that species perceive the perturbation. We will discuss this term in detail in following sections.~~, a property known to have potentially strong, and unintuitive effects on species dynamics (Ripa and Ives, 2003).

~~Not all dynamical systems written as~~ For the fluctuations of species abundance in eq. (1) ~~lead to stationary fluctuations. For this to be the case~~ to be stationary, the equilibrium state (N_i) must be stable. More technically, the eigenvalues of the community matrix A must ~~satisfy the stability criterion: all its eigenvalues must~~ have negative real part (May, 1973a; Gurney and Nisbet, 1998). The ~~eigenvalue with~~ maximal real part determines the slowest long-term rate of return to equilibrium following ~~any weak~~ a pulse perturbation. This rate is a commonly used stability measure in theoretical studies~~. We ~~; we call it *asymptotic resilience* and denote it by $\mathcal{R}_\infty$ (Arnoldi et al., 2016b). ~~It will serve as a reference~~To illustrate the connections between stability concepts, we will compare asymptotic resilience to measures of variability.

Perturbation type

The ~~dependency with species biomass of the perturbation term (??) models a~~ perturbation term in eq. (1) represents the direct effect that a perturbation has on the abundance of species i. It consists of two terms: some power α of $\sqrt{N_i}$, and a species-specific term $\sigma_i \xi_i(t)$. The latter is a function of the perturbation itself, and of traits of species i that determine how individuals of that species perceive the perturbation. The former defines a statistical relationship between a perturbation's direct effects and the mean ~~biomass~~ abundance of perturbed species. ~~This relationship allows to consider many, and very distinct~~, It allows us to consider ecologically distinct sources of variability (Fig. 2).

When individuals of a given species respond in synchrony to a perturbation, ~~its direct effect will scale roughly linearly with~~ the direct effect of the perturbation will be proportional to the abundance of ~~that~~ the perturbed species, thus a value of α ~~in eq. (??),~~ close to 2 (Lande et al., 2003). We call this type of perturbation *environmental* as fluctuations of environmental variables typically affect all individuals of a given species, leading, ~~for instance,~~ e.g. to changes in the population growth rate ~~(Lande et al., 2003).~~ (May, 1973b).

If individuals respond incoherently, ~~however,~~ e.g., some negatively and some positively, the direct effect of the perturbation ~~on that species biomass~~ will scale sublinearly with ~~that~~ species abundance. For instance, demographic stochasticity can be seen as a perturbation resulting from the inherent stochasticity of birth and death events, which are typically assumed independent between individuals. In this case $\alpha = 1$, and we thus call such type *demographic* ~~(Haegeman and Loreau, 2011). The power-law relationship can also encode~~ (Lande et al., 2003).

We can also consider purely exogenous perturbations, such as the random removal or addition of individuals. ~~This can be done by setting~~ In this case $\alpha = 0$. We call ~~the latter~~

~~of the~~ such perturbations *immigration*~~type~~ -type but stress that actual immigration events ~~are not necessarily of this type~~ do not necessarily statisfy this condition (e.g., they can be density-dependent).

~~With the expression (??) we can thus consider a continuum of perturbation type , from purely exogenous stochasticity (~~ Furthermore, because we focus on zero-mean perturbations, perturbations of this type contain as much *emigration* than immigration. The reasoning behind this nomenclature is that, in an open system, fluctuations of an otherwise constant influx of individuals (immigration flux) would correspond to an immigration-type ~~α = 0), to environmental perturbations (α = 2) , via demographic stochasticity (α = 1) . Although~~ perturbation.

More generally, eq. (1) with $\alpha \in [0, 2]$ can describe a continuum of perturbation types. Note that, although not unrelated, ~~the statistical relationship (??)~~ such a statistical relationship between a perturbation's direct effects and the ~~biomass~~ abundance of perturbed species is not equivalent to Taylor's (1961) law. The latter is an empirically observed power-law relationship between the variance and mean of population ~~biomass time-series.~~ fluctuations. Hence, in contrast to the perturbation type α, the exponent of Taylor's law depends on community dynamics, e.g., on species interactions (Kilpatrick and Ives, 2003). We will come back to this point below and in the Discussion.

Community response vs perturbation intensity

For a given community, a stronger perturbation will ~~naturally~~ lead to stronger fluctuations. ~~This could reveal non-linear dynamical properties of the system considered, but in~~ A disproportionate increase in their amplitude as perturbation intensity changes would reveal nonlinearity in the dynamics (Zelnik et al., 2019). In a linear setting, ~~by definition, this is not~~

12

~~the case. Since we placed ourselves in this setting, to see in temporal variability a reflection~~ ~~of a community's dynamical properties, we must control~~ however, such effects cannot occur and there is only a linear dependency on perturbation intensity. This trivial dependency can be removed by controlling for perturbation intensity. We now ~~discuss~~ illustrate how to do so, for a ~~simple~~ given definition of variability.

~~By linearity, the~~ In our setting, fluctuations induced by white-noise forcing are normally distributed, thus fully characterized by their variance and covariance. It ~~thus makes sense~~ is therefore natural to construct a measure of variability based on the variance of species ~~biomass. To allow a comparison between communities of different diversity, a simple choice~~ ~~is to consider the average variance,~~ time-series. To compare variability of communities with different species richness we will measure their average variance:

$$\sigma_{\text{out}}^2 = \frac{1}{S} \sum_i \text{Var}(N_i(t)). \tag{2}$$

~~We will discuss this choice further, but for now, from this definition of community response,~~ ~~we~~ In empirical studies, variability is often associated to an ecosystem function (primary productivity, ecosystem respiration, etc). This amounts to measuring the ecosystem response along a direction in the space of dynamical variables. In Appendix B we explain how considering the average variance amounts to taking the expected variance along a random choice of direction of observation. In this sense, eq. (2) represents the variance of a "typical" observation.

We now wish to remove the trivial effect of perturbation intensity ~~.~~ from eq. (2). Let us start from a one-dimensional system ~~$dx/dt = -rx + \sigma W(t)$~~ $dx/dt = -\lambda x + \sigma \xi(t)$. Its stationary variance is ~~$\sigma_{\text{out}}^2 = \frac{\sigma^2}{2r}$. We see here the contribution~~ $\sigma_{\text{out}}^2 = \frac{\sigma^2}{2\lambda}$. Here we see the combined effect of perturbation σ^2 and dynamics ~~r in determining the response. Here, a natural choice~~

13

~~for perturbation intensityis~~ λ, leading us to define σ^2 as measure of perturbation intensity. For species-rich communities, ~~if we define the intensity of a perturbation~~ we define perturbation intensity as the average intensity per species, that is, using the species-specific intensities σ_i^2:

$$\sigma_{\text{in}}^2 = \frac{1}{S} \sum_i \sigma_i^2. \tag{3}$$

When increasing all species-specific perturbation intensities by a factor c, both σ_{in}^2 and σ_{out}^2 increase by the same factor. To remove this ~~trivial dependency from our measure of variability, we consider the ratio~~

$$\mathcal{V} = \sigma_{\text{out}}^2 / \sigma_{\text{in}}^2,$$

~~from which we deduce a measure of stability,~~ linear dependence, we define variability as

$$\mathcal{V} = \frac{\sigma_{\text{out}}^2}{\sigma_{\text{in}}^2}, \tag{4}$$

i.e., as the average species variance relative to perturbation intensity (see Ives et al., 2003 for a similar definition of variability). Generalizing previous work (Arnoldi et al., 2016b; Arnoldi and Haegeman to an arbitrary perturbation type, we construct *invariability* ~~, defined as~~ as

$$\mathcal{I} = 1/2\mathcal{V} \tag{5}$$

The factor $1/2$ ~~in the definition of invariability allows it~~ allows $\mathcal{I}$ to coincide, for simple systems, with asymptotic resilience ~~. It is the case~~ (Arnoldi et al., 2016b). In particular, for the one-dimensional example considered above ~~, where $\mathcal{R}_\infty = r$ and, in response to immigration-type perturbations, $\mathcal{V} = 1/2r$, so that $\mathcal{I} = r = \mathcal{R}_\infty$~~ for which $\mathcal{R}_\infty = \lambda$, we do have $\mathcal{V} = 1/2\lambda$ and thus $\mathcal{I} = \lambda = \mathcal{R}_\infty$.

14

In empirical studies, temporal variability is often associated to a given observable ecosystem function (primary productivity, respiration, basal or top species biomass, and so forth). In our setting, this amounts to measuring the ecosystem response along a direction in the space of dynamical variables. In Appendix B we explain considering average variance to define variability, amounts to taking the expected variance along a random choice of direction of observation. In this sense, eq. (2) represents a "typical" observation. We will come back in the Discussion (and Appendix I) to other variability metrics that have been used in empirical studies, such as coefficient of variation of total biomass or populations.

Variability spectraPerturbation directions and the variability distributions

Once intensity is controlled for, perturbations can still differ in how their intensity is distributed and correlated across species. For example, weWe want to be able to model the fact that species with similar physiological traits ought towill be affected in similar ways by, say, temperature fluctuations, whereas individuals from dissimilar species may react in unrelated, or even opposite, ways (Ripa and Ives, 2003). We will thus study the effect of changing,, at fixed intensity, the covariance structuresthe covariance structure of the perturbation terms, i.e.changing the , the effect of the *direction* of perturbations, and not their overall intensity. .Spanning the set of all perturbation directions will naturally define a whole range of community responseresponses. Assuming some probability distribution over this set consequently defines translates into a probability distribution over the set of ensuing responses. We call this latter distribution the *variability spectrum* responses, i.e., a variability distribution (see Fig. 2). We will typically assume all perturbation directions to be equiprobable, but our framework allows different choices of prior. FnallyFinally, spanning the set of perturbation types then reveals a continuous family of *variability spectra* (blue , green, and red distributions

15

family of variability distributions. In Fig. 2 we show three archetypal elements of this family, corresponding to $\alpha = 0$ (blue distribution), $\alpha = 1$ (green distribution) and $\alpha = 2$ (red distribution).

For each distribution we consider two complementary statistics: mean- and worst-case responses. In Appendix C and D we prove that the worst-case response is always achieved by a perfectly coherent perturbation, i.e., a perturbation whose direct effects on species are not independent, but on the contrary, perfectly correlated in time. We derive explicit formulas to compute the worst-case variability from the community matrix and species equilibrium abundances, see eqs. (C2, D5). The mean-case scenario, on the other hand, is defined with respect to a prior over the set of perturbation directions. For the least informative prior, we prove in Appendix C and D that a perturbation affecting all species independently but with equal intensity, realizes the mean-case response. This provides a way to compute this response from the community matrix and the species abundances, given in eqs. (C3, D6).

Variability patterns for two-species community

Before considering complex communities, let us illustrate our variability framework on the following elementary example, in the form of a 2×2 community matrix

$$A = \begin{pmatrix} -1 & 0.1 \\ -4 & -1 \end{pmatrix}. \tag{6}$$

perturbation type → perturbation direction → community response → observation → variability distribution

Example:
one (environmental) perturbation leads to *one* value of variability

P$_1$ R$_1$ $\mathcal{V}_1$

frequency — 1 $\mathcal{V}_1$
Variability($\mathcal{V}$)

different perturbation directions lead to different responses

mean-case
worst-case

Environmental-type: Coherent response of individuals

Demographic-type: Incoherent response of individuals

Immigration-type: Random number of individuals removed or added

P$_1$ P$_2$ P$_3$ P$_n$

R$_1$ R$_n$

$\mathcal{V}_1$ $\mathcal{V}_n$

frequency

sampling the intensity of responses leads to a distribution of variability values
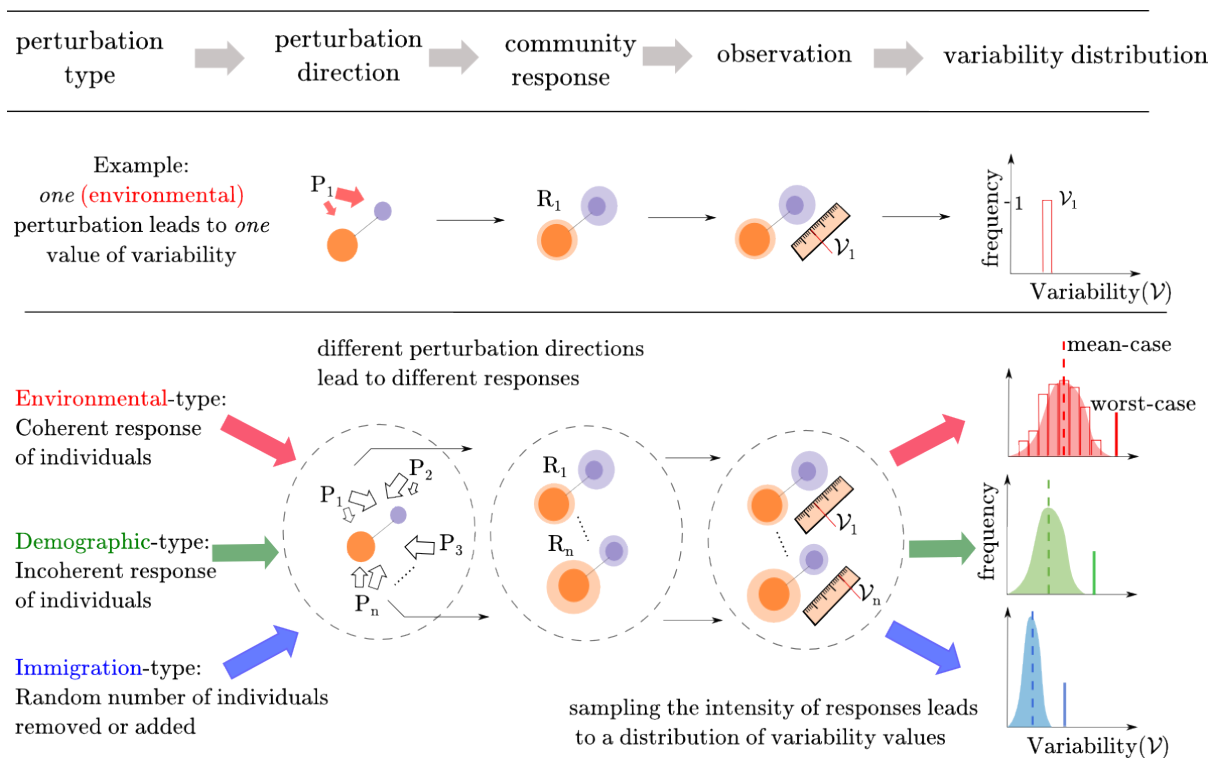
Variability($\mathcal{V}$)

Figure 2: ~~The~~ A theoretical framework for variability~~spectrum as a function of perturbations type~~. ~~Top row: as previously illustrated in Fig. 1B, a variability measurement of a community (here two species, represented~~ Perturbations are characterized by ~~the orange and purple discs~~their type, ~~whose diameter represent abundance) is a~~ ~~function of both~~ statistical relationship between the ~~dynamics~~ direct effect of ~~this community~~ perturbations and the ~~environmental perturbation P_1 that it faces. Subsequent rows: we will consider various types~~ abundance of ~~perturbations ranging from environmental to immigration~~perturbed species. For a given type and fixed intensity, ~~via demographic stochasticity (see main text for~~ there remains a ~~precise definition). We eliminate the dependence on specific features~~ whole set of covariance structure of ~~perturba-tions (i.e .~~their direction~~, see main text~~) that will be transformed by ~~sampling many perturbations leading to~~ community dynamics into a whole ~~spectrum~~ set of ~~response~~community responses, ~~called the variability spectrum~~i.~~Considering all types~~e., various covariance structure of ~~perturbations then reveals~~species stationary time series. A sampling of those responses, ~~for~~ measured here as an average variance, leads to a ~~given system~~variability distribution, one for each perturbation type. Spanning all perturbation types leads to a family of variability ~~spectra~~distributions (in blue green and red in the rightmost column). We derive analytical formulas for the largest value (worst-case scenario) and for the mean value (mean-case scenario).

This matrix defines a ~~linear~~ <u>linear</u> dynamical system that could represent a predator-prey community, with the first species benefiting from the second at the latter's expense. ~~It is stable with asymptotic resilience~~ <u>Its asymptotic resilience is</u> $\mathcal{R}_\infty = 1$. Let us suppose that the ~~biomass of the~~ prey, N_2 (second row<u>/column</u> of A) is 7.5 times ~~larger than the one of~~ <u>more abundant than</u> its predator, N_1 (first row<u>/column</u> of A) and consider stochastic perturbations of this community, as formalized in eq. (1).

In Fig. 3 we represent ~~, for any given type,~~ the set of perturbation directions as a disc, ~~every point of the disc corresponding to~~ <u>in which every point is</u> a unique perturbation direction (see Appendix E for details). The effect of a perturbation on a community ~~can be~~ <u>is</u> represented as a color~~, darker tones implying larger response~~<u>; darker tones imply larger responses</u>, with the baseline color (blue, green or red) recalling the perturbation type ($\alpha = 0, 1, 2$, respectively). Points at the ~~borders of the discs correspond to perfectly correlated perturbations, so that the largest response is achieved from such perturbations:~~ <u>boundary of the disc correspond to coherent perturbations, which have the potential to generate the largest (but also the smallest) variability. This is why</u> the color maps ~~represented in~~ <u>of</u> Fig. 3 ~~which are always darkest on the borders of the disc.~~

~~We see in the second row of Fig. 3 that variability not only~~ <u>take their extreme values at the boundary. We see that variability strongly</u> depends on the perturbation ~~directions, but~~ <u>direction, and</u> that this dependence is ~~in turn~~ strongly affected by the perturbation type. For immigration-type perturbations (in blue) variability is largest when perturbing the predator species most strongly (the least abundant species in this example). For demographic-type perturbations (in green) perturbations that equally affect the two species but in opposite ways achieve the largest variability. For environmental-type perturbations (in red) variability is largest when perturbing the prey species (the most abundant species in this example). For all types we see that positive correlations between the components of the perturbation (<u>i.e.,</u>

18

moving upwards on the disc) reduce variability (see Ripa and Ives, 2003 for related results).

Thus, in general, a given community cannot be associated to a single value of variability. Depending on the type of perturbations causing variability, different species can have completely different contributions. This stands in sharp contrast with asymptotic resilience $\mathcal{R}_\infty$, which associates a single stability value to the community. Although we know from previous work (Arnoldi et al., 2016b) that the smallest invariability value in response to immigration-type perturbations will always be smaller than $\mathcal{R}_\infty$, in general (i.e., any perturbation type and/or any perturbation direction) there is, a priori, no reason to expect a relationship between invariability and asymptotic resilience.

Generic variability patterns in complex communities

The dimensionality of variability will be larger in communities comprised of many species, as their sheer number, S, increases the dimension of the perturbation set quadratically. Yet, when species interact, a generic structure can emerge from ecological assembly, revealing a simple relationship between variability and the abundance of perturbed species. To show this, we first generate a pool of 50 species following Lotka-Volterra dynamics and let the system settle to an equilibrium.
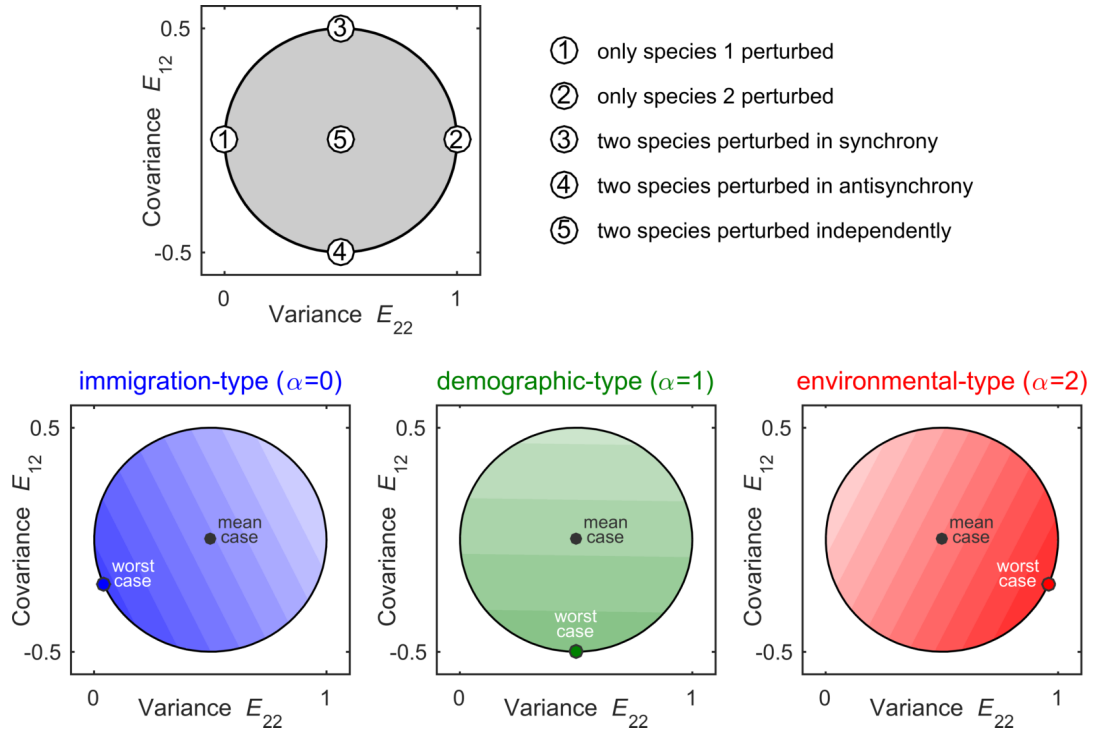
Figure 3: Variability depends on perturbation direction and perturbation type. Top panel: For a two-species community the set of all perturbation directions can be represented graphically as a disc (shaded in gray), with the variance of the perturbation term $\xi_2(t)$ on the x-axis and the covariance between $\xi_1(t)$ and $\xi_2(t)$ on the y-axis. Some special perturbation directions are indicated (numbers 1 to 5, see also Appendix E). ~~Panels A-C~~Bottom panels: We consider a predator-prey system; the community matrix A is given by eq. (6), and the ~~equilibrium biomass for the predator~~ prey (species ~~1~~2) is 7.5 ~~times smaller~~ more abundant than ~~for the prey~~ its predator (species ~~2~~1). The induced variability depends on the perturbation directions (darker colors indicate larger variability), and this dependence in turn depends on the perturbation type α. ~~A:~~ For immigration-type perturbations ($\alpha = 0$, in blue) variability is largest when perturbing species 1 most strongly. ~~B:~~ For demographic-type perturbations ($\alpha = 1$, in green) perturbations that affect the two species equally strongly but in opposite ways achieve the largest variability. ~~C:~~ For environmental-type perturbations ($\alpha = 2$, in red) variability is largest when perturbing species 2 most strongly. Notice that the worst case is always achieved by perturbations lying on the edge of the perturbation set. Such perturbations are ~~fully~~ perfectly correlated (see main text and Appendix E).

20

We randomly draw species dynamical traits, starting with a configuration in which mean interspecific interaction strength is one tenth of the strength of species self-regulation, with a comparable variation around this mean (a complete description of the nonlinear model is given in Appendix F ~~for details). Importantly, such communities exhibit uneven abundance distributions, thus allowing perturbation types to play an important role in a community's variability~~and Matlab simulation code is available as supplementary material). Some species would go extinct during assembly, but no limit cycles, chaotic behavior or multi-stability were observed.

In this species-rich ~~communities~~ context, the perturbation set cannot be represented ~~as in the two-dimensional example of Fig. 3. What is possible and enlightening, however, is to~~ exhaustively. We therefore focus on the effect of a specific subset of perturbations, those ~~that affect~~ affecting a single species. ~~By superposition, this allows the study of perturbation~~ Linear combinations of these perturbations will span all scenarios in which species are affected independently, but ~~it excludes~~ exclude scenarios in which ~~species~~ they are perturbed in systematically correlated or anti-correlated way[2]. In Fig. 4 we consider a ~~random community of 40 interacting~~ community of $S = 40$ coexisting species. We ~~order species according to their abundance and~~ plot the variability induced by ~~perturbing them. We observe the following patterns:~~

~~(i) When~~species-specific perturbations (of various types) against the abundance of perturbed species.

The leftmost panel shows a negative unit slope on log scales: when caused by immigration-type perturbations, variability is inversely proportional to the abundance of ~~the perturbed species(leftmost panel). In other words, randomly~~ perturbed species. Randomly adding and

---

[2]In terms of the geometrical representation of Fig. 3, this amounts to restricting to the equator of the perturbation disc

removing individuals from common species generates less variability than when the species is rare. In fact, the worst-case scenario corresponds to perturbing the rarest species. Worst-case invariability is close to asymptotic resilience, which corroborates previous findings showing that the long-term rate of return to equilibrium is often associated to rare species (Haegeman et al., 2016; Arnoldi et al., 2018). On the other hand, the middle panel of Fig. 4 shows that, in response to demographic-type perturbations, variability is independent of perturbed species' abundance. Finally, the rightmost panel shows a positive unit slope on log scales: when caused by environmental-type perturbations, variability is proportional to the abundance of perturbed species. The worst case is thus attained by perturbing the most abundant one. Despite being more stable than rare ones (they buffer exogenous perturbations more efficiently, see left-hand panel), common species are more strongly affected by environmental perturbations, and can thus generate the most variability.

Those patterns are not coincidental but emerge from species interactions. In their absence, other patterns can be envisioned. This is because, without interactions, the response to a species-specific perturbation involves the perturbed species only. The variability-abundance relationship is then $\mathcal{V} = N^\alpha/2r$, with $N = K$. If r and K

22
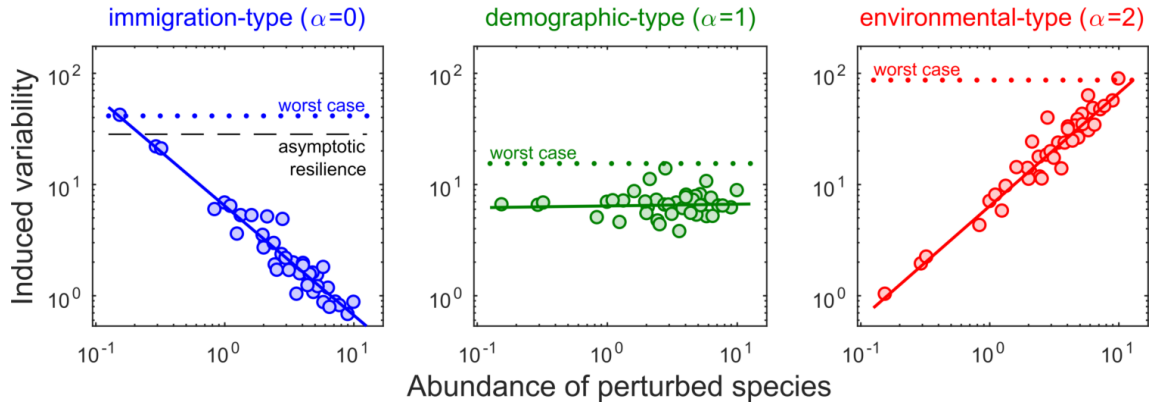
Figure 4: The contribution of abundant and rare species to variability. We consider a community of $S = 40$ species, and look at the variability induced by perturbing a single species, whose ~~abundnace~~ abundance is reported on the x-axis. Left: When caused by immigration-type perturbations ($\alpha = 0$), variability is inversely proportional to the abundance of the perturbed species (notice the log scales on both axis). The worst case is achieved by perturbing the rarest species, and is determined by asymptotic resilience (more precisely, it is close to $1/2\mathcal{R}_\infty$). Middle: For demographic-type perturbations ($\alpha = 1$), variability is independent of the abundance of the perturbed species. The worst case is not necessarily achieved by focusing the perturbation on one particular species. Right: For environmental-type perturbations ($\alpha = 2$), variability is directly proportional to the abundance of the perturbed species. The worst case is attained by perturbing the most abundant one.

are statistically independent in the community (top-left panel in Fig. 5), this yields a different scaling than the one seen in Fig. 4. In the case of an r-K trade-off (i.e., species with larger carrying capacities have slower growth rate), abundant species would be the least stable species (bottom-left panel in Fig. 5, in blue) which is the opposite of what the leftmost panel of Fig. 4 shows. However, as interaction strength increases (from left to right in Fig. 5), we see emerging the relationship between abundance and variability of Fig. 4, regardless of the choice made for species growth rates and carrying capacities. We explain in Appendix G why this reflects a generic, limit-case behavior of complex communities. It occurs when species abundances, due to substantial indirect effects during assembly, become only faintly determined by their carrying capacities[3]. Importantly, our example demonstrates that this limit can be reached even for relatively weak interactions (recall that in Fig. 4 and in the right-hand panels of Fig. 5, the interspecific interaction strengths are ten times smaller than the intraspecific ones).

Although we considered a specific section of the perturbation set, the response to single-species perturbations of immigration and environmental types can still span the whole variability distribution, from worst-case (rarest and most abundant species perturbed, respectively) to mean- and best-case scenarios (most abundant and rarest species perturbed, respectively). For

---

[3]The slope of a linear regression between these quantities on logarithmic scales approaches zero.

demographic-type perturbation the situation is more subtle as the response is independent of species abundance, and, in general, extreme scenarios will be associated to temporally correlated perturbations affecting multiple species.

The variability-abundance patterns shown in Figs. 4 and 5 should not be confused with Taylor's (1961) law, a power-law relationship between a species' variance and its mean abundance. In fact, the variability-abundance pattern is *dual*[4] to Taylor's law, it represents the community response to single-species perturbations instead of that of individual species to a community-wide perturbation.

Implications for the ~~diversity-stability~~ diversity-invariability relationship

~~We may now explore the underlying role of the above patterns in~~ To illustrate some implications of the generic variability-abundance pattern, we now propose to revisit the diversity-stability ~~relationships. Gradually~~ relationship, with stability quantified as invariability $\mathcal{I}$. For a given size of the species pool, we randomly sample species dynamical traits to assemble a stable community. ~~By~~ increasing the size of the ~~species pool and drawing random growth and interaction parameters, we generate many different communities of various diversity from the same class of random Lotka-Volterra models as above. For every community~~ pool we generate communities of increasing species richness S. For each community, we uniformly sample the boundaries of its perturbation set by drawing 1000 fully correlated perturbations (i.e., those that can realize the maximal response), of a given type. We compute the bulk of ~~its variability spectra (10th to 90th percentiles~~ responses to uniformly drawn perturbations) together with

---

[4]Dual in the sense that the level of organization of observation and response are reversed. For Taylor's law the perturbation acts at the community level, and is observed at the population level. In the patterns described here, the perturbation acts at the population level, while the observation is at the community level.

25
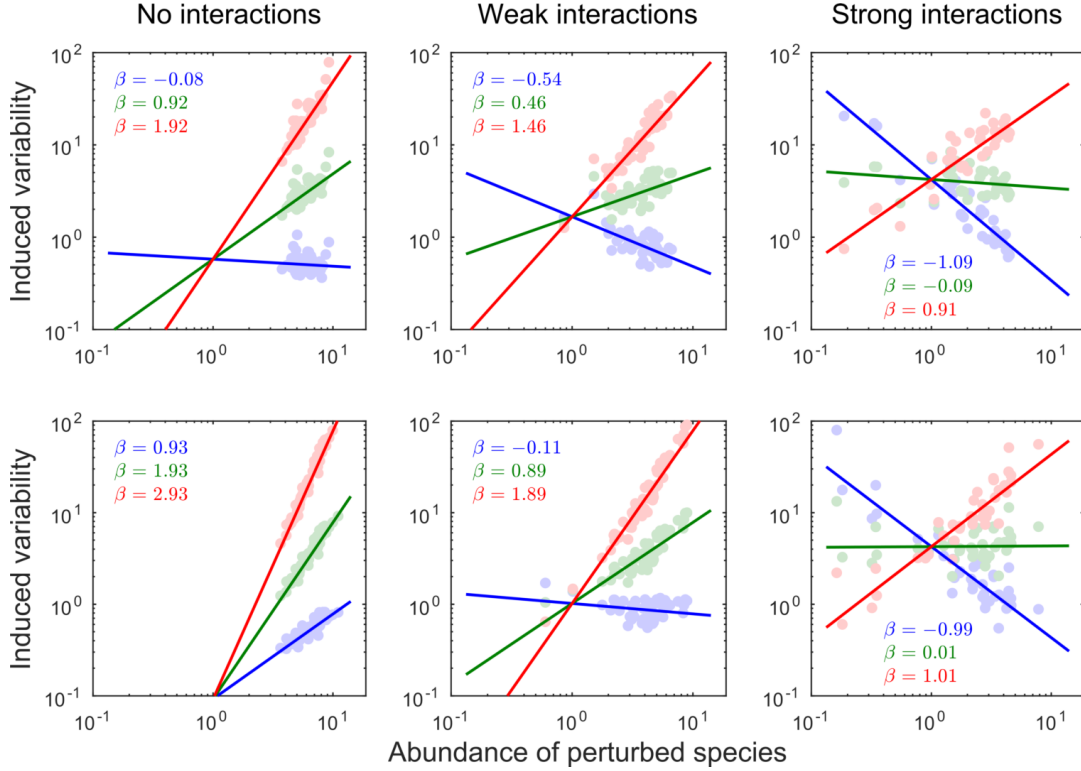
Figure 5: The emergence of the ~~role of species abundance in a community's variability~~ variability-abundance pattern (same procedure as in Fig. 4). Top row: intrinsic growth rates r and carrying capacities K are sampled independently. Bottom row: Species satisfy a r~~vs~~ K trade-off $(r \sim 1/K)$. Colors correspond to the three perturbation types: $\alpha = 0$ (blue), $\alpha = 1$ (green) and $\alpha = 2$ (red). The value β reported in each panel corresponds to the exponent of the fitted relationship $V_i \propto N_i^{\beta}$ for each perturbation type. As interaction strength increases (left to right) we see emerging the relationship between abundance and variability described in Fig. 4, i.e., $\beta = \alpha - 1$. Thus when species interactions are sufficiently strong, variability always ends up being: (blue) inversely proportional, (green) independent and (red) directly proportional to the abundance of the perturbed species. Note that such relationships differ from Taylor's law: they represent an average community response to individual species perturbations, whereas Taylor's law deals with individual species responses to a perturbation of the whole community.

the resulting invariability distribution (5 to 95 percentiles), as well as its mean and extreme realized values. We also compute theoretical predictions for mean- and worst-case scenarios, ~~as well as asymptotic resilience . Following eq. (5) we measure stability as invariability. For a given sequence of communities, we observe three qualitatively different stability-diversity relationships (Fig. 6).~~ and asymptotic resilience $\mathcal{R}_\infty$.

~~(i) In the~~ The leftmost panel of Fig. 6 ~~, invariability is defined from the response to~~ shows a negative relationship between immigration-type ~~perturbations. It is an exponentially decreasing function of diversity (notice the log scale on the y-axis).~~ invariability and species richness. Asymptotic resilience and worst-case invariability mostly coincide, with a decreasing rate roughly twice as large as ~~the one~~ that of the mean case. ~~Here, clearly, diversity begets instability (May, 1972).~~

~~(ii) In the middle panel , defining stability from the response to demographic-type perturbations gives~~ The middle panel suggests a different story. Mean-case demographic-type invariability stays more or less constant whereas the ~~worst-case diminishes at an exponential rate with diversity. The rate of decrease is however four times smaller then of asymptotic resilience. Here the~~ worst case diminishes with species richness, although much more slowly than $\mathcal{R}_\infty$. The relationship between diversity and stability ~~appears to be ambiguous.~~

~~(iii)~~ is thus ambiguous. In the rightmost panel ~~, environmental perturbations yield an increase of all realized~~ we see an increase in all realized environmental-type invariability values with ~~diversity, in sharp contrast with the trend followed by asymptotic resilience.~~ species richness, showcasing a positive diversity-stability relationship.

~~Thus, the spread of biomass across more and more species as diversity increases has opposite effects on variability depending on the type of perturbation causing it. Assuming interactions are independent of species richness, the limit of relatively strong interactions described in~~ The generic limit that yields the variability-abundance patterns of Figs. 4 and 5

27

is the one towards which a community of increasing ~~diversity~~ complexity – *sensu* May (1972)
– will tend. This explains why, in the case of immigration-type perturbations, the increas-
ing rarity of many species as S increases is a source of instability. ~~Indeed, at high enough~~
~~diversity each species genericaly contributes to variability proportionally~~ Species contributions
to variability become proportional to the inverse of ~~its abundance (as in the~~ their abundance
(first panel of Fig. 4)~~. The~~, and the worst-case scenario ~~thus~~ follows the abundance of the
rarest species, which rapidly declines with ~~diversity. Furthermore, as~~ species richness. As
detailed in Appendix H, mean-case invariability ~~will scale as an average abundance which~~
~~also,~~ scales as the average species abundance, which also typically decreases with ~~diversity.~~
S.

The responses to demographic perturbations, on the other hand, are not determined by
any specific species abundance class (~~as in the middle~~ second panel of Fig. 4)~~. As we argue~~
~~in the Discussion, this is because demographic variability generically reflects the collective~~
~~response of communities, i. e. an inherent property of the interaction network, and not~~
~~species abundances.~~, so that no simple expectations based on typical trends of abundance
distributions can be deduced.

~~In~~ We recover a simpler behavior when looking at the response to environmental-type
~~perturbations, it~~ perturbation. It is now abundant species that ~~mostly contribute to variability~~
~~with the worst-case scenario following the abundance of the most common species (as in~~
~~the leftmost~~ drive variability (rightmost panel of Fig. 4). ~~Mean-case variability (and not~~
~~its inverse)~~ As explained in Appendix H, mean-case invariability now scales as ~~an average~~
~~abundance. Here the number of rare species matters for~~ the *inverse* of an average species
abundance. The latter typically declines with S explaining the observed increase of mean-
case ~~variability but not their individual abundance~~ invariability.

~~There is thus close connection~~ In all panels of Fig. 6, the bulk of invariability stays close to

28

the mean- while moving away from the worst-case. This is because the worst-case corresponds to a single direction of perturbation met with the strongest response, a fine-tuned perturbation which becomes increasingly unlikely to be picked at random as S increases.

There is an analogy to be made between stability and diversity~~metrics~~. As has been said about diversity metrics (e.g., species richness, Simpson index or Shannon entropy), different invariability measures ~~"differ in their propensity to include or to exclude the relatively rarer species"~~ *"differ in their propensity to include or to exclude the relatively rarer species"* (Hill, 1973). In this sense, ~~they~~ different invariability measures can probe different dynamical aspects of a same community, with potentially opposite dependencies on a given ecological parameter of interest.

~~In all panels of Fig. 6 the bulk of invariability stays close to the mean-case while moving away from its worst-case value. This is because the worst-case scenario corresponds to a single direction of perturbation met with the strongest response, i.e., a fine-tuned perturbation exploiting specific dynamical interdependencies between species that ought to become less and less likely to pick at random as diversity increases. The mean-case is by definition more representative of generic perturbations, allowing for compensatory effects between species.~~

Discussion

Summary of results

Because it is empirically accessible using simple time-series statistics, temporal variability is an attractive facet of ecological stability. ~~Yet~~ But there are many ways to define variability in models ~~, or to measure it on~~ and empirical data, a proliferation of definitions reminiscent of the proliferation of definitions of stability itself (Grimm and Wissel, 1997). ~~From an empirical~~

29
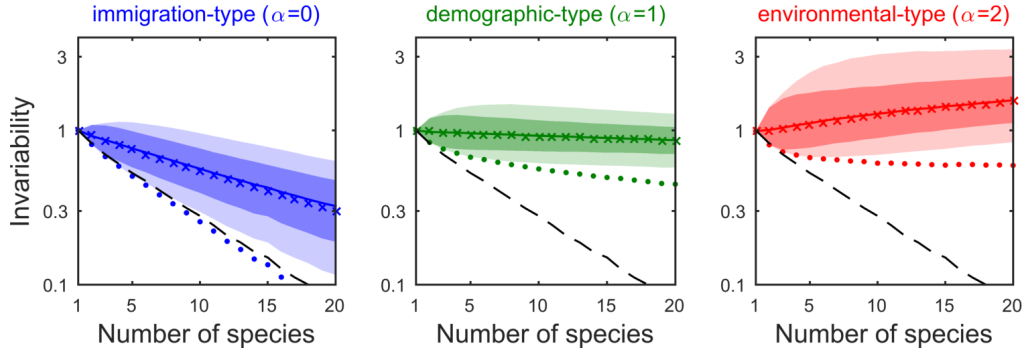
Figure 6: Different perturbation types yield contrasting ~~diversity-stability~~ diversity-invariability relationships. We generated random ~~Lotka-Volterra competitive~~ communities of increasing ~~diversity~~ species richness S and computed their invariability ~~(log scales on both axes). We computed the invariability for~~ distribution in response to 1000 ~~perturbation directions; full~~ random perturbations. Full line: median ~~over perturbations~~ invariability, dark-shaded region: 5th to 95th percentile, light-shaded region: minimum to maximum realized values. The ×-marks correspond to the analytical approximation for the median~~invariability~~, the dots to the analytical formula for the worst-case~~invariability~~. ~~As a reference, the dashed~~ Dashed line ~~follows~~ is asymptotic resilience ~~along the diversity gradient~~ $\mathcal{R}_\infty$. For immigration-type perturbations ($\alpha = 0$, blue) diversity begets instability, with ~~asymptotic resilience closely~~ $\mathcal{R}_\infty$ following worst-case invariability. For demographic-type perturbations ($\alpha = 1$, green) ~~mean-case invariability does not vary with diversity~~ the trend is ambiguous. For environmental-type perturbations ($\alpha = 2$, red) ~~stability increases~~ all realized values of invariability increase with ~~diversity~~ S.

Variability measurements often depend, not only on the system of interest, but also on external factors that act as disturbances, which makes it difficult to relate variability to other stability concepts. These caveats constitute important obstacles toward a synthetic understanding of ecological stability, and its potential drivers (Ives and Carpenter, 2007).

We proposed to consider variability as a way to probe and measure an ecosystem's response to perturbations, thus revealing inherent dynamical properties of the perturbed system. We did not seek for an optimal, single measure of variability but, on the contrary, we accounted for a vast set of perturbations, leading to a whole distribution of responses. We focused on the worst- and mean-case values of this distribution as functions of species abundance, their interactions, and the *type* of perturbations that generates variability.

A perturbation type characterizes a statistical relationship between its direct effect on a population and the latter's abundance. We distinguished between environmental perturbations, whose direct effects on populations scales proportionally to their abundance; demographic perturbations, whose direct effect on populations scales sublinearly to their abundance; and purely exogenous perturbations, representing random addition and removal of individual, independent of the size of the perturbed population (immigration-type). Controlling for perturbation type and intensity, we considered all the ways this intensity can be distributed and correlated across the species of a community. Since each perturbation type defines a

~~variability spectrum, the notion of variability unfolds as a continuous family of *variability spectra.*~~ species.

~~On random Lotka-Volterra community models we found that~~ After having described a general (linear) theory for variability, ~~depending on perturbation type , both common or~~ which emphasizes its highly multidimensional nature, we turned our attention towards species-rich communities assembled by random (nonlinear) Lotka-Volterra dynamics. Because of the sheer number of species contained in such communities ($S \approx 40$ in our examples), we could have expected the dimensionality of perturbations and responses to be so large that variability distributions would be too complex and broad to be clearly described. However, the process of assembly allowed for a simple behavior to emerge: a generic relationship between variability and the abundance of individually perturbed species. In essence, this pattern predicts that species ability to buffer exogenous perturbations is inversely proportional to their abundance. In conjunction to this simple pattern, the type of perturbation will then determine the individual contributions of species to the variability distribution, so that both common and rare species can determine variability. This is reminiscent of diversity measures (Hill, 1973)~~:~~, some of which (e.g., species richness) are sensitive to the presence of rare species, while others are mostly indicative of ~~abundant ones~~ the distribution of abundant species (e.g., Simpson diversity index). ~~For a sequence of model communities of increasing species richness, that~~

These connections with different diversity metrics can explain contrasting trends in invariability as a function of species richness. Since immigration-type perturbations ~~gives a prominent role to rare speciesexplains the negative diversity-stability observed in Fig. 6. It reflects the growing vulnerability~~ mostly affect rare species, they lead to a negative diversity-invariability relationship, reflecting a growing number and rarity of rare species~~pushed towards the edge of extinction as diversity increases. Such rare species do not regulate well immigration type~~

32

~~perturbations, which leads them to determine the largest values of the variability spectrum. More generally, the contribution of species to variability generically scales as the inverse~~ . On the other hand, in response to demographic perturbations, species contributions to variability can be independent of their abundance~~(Fig. 4), which leads to a proportional relationship between mean-case invariability and average abundance, the latter typically declining with diversity(Appendix H). When caused by demographic-type perturbations, a species contribution to variability is generically independent of its abundance, allowing for potentially ambiguous diversity-stability patterns~~ . ~~By contrast, common species are generically the most stable, yet~~ In this case, variability is not expected to follow trends in diversity, so that diversity-invariability patterns can be less predictable and harder to interpret. Finally, although common species buffer exogenous perturbations efficiently, they are also the most affected by ~~environmental perturbations, allowing them to drive the larger values of the variability spectrum. More generally, the contribution of species to variability is generically proportional to their abundance (Fig. 4) which in turns leads to~~ environmental-type perturbations. This can lead to a proportional relationship between average abundance and mean-case ~~variability (and not its inverse as was the case for immigration-type), typically leading~~ invariability, and hence to a positive ~~diversity-stability relationship.~~ diversity-invariability relationship.

~~Of the two patterns described—emerging role of abundance and~~

Implications for empirical patterns

Our theoretical models show wide variability distributions. These distributions would become even wider when accounting for nonlinear system dynamics and temporally autocorrelated perturbations. Therefore, we also expect a large dispersion of empirical variability data, i.e.,

33

when the variability of the same system is measured repeatedly. For certain applications it might be sufficient to restrict to a particular perturbation regime, but in order to detect in variability an inherent stability property of a system, i.e. a property that is not bound to a specific environmental context (see Fig. 1), one must describe of the spread of variability.

To do so, the most direct approach consists in observing the same community under multiple environmental conditions. With relatively few observations, one can estimate the mean and spread of the response distribution. There is, however, more information to be extracted from a time series than a single variability value. If high-quality time series are available, it might be possible to infer linear model dynamics, which can then be used to compute stability properties (Ives et al., 2003), and in particular, variability distributions.

We showed that species abundances greatly affect variability distributions. This new insight has broad consequences. For example, it has been reported that ecosystem-level and population-level stability tend to increase and decrease, respectively, with increasing diversity (Jiang and Pu, 2009; Campbell et al., 2011). Ecosystem-level stability is often quantified based on the variability of total biomass, which gives, by construction, a predominant weight to abundant species. On the other hand, averages of single-species variabilities have been used to measure population-level stability (Tilman, 1996). These averages are strongly affected, and can even be fully determined, by rare, highly variable species (Haegeman et al., 2016). Thus, here as well as in our theoretical results (Fig. 6), stability metrics governed by common, or rare, species tend to generate respectively positive and negative diversity-stability relationships – the first is the most robust to modeling choices or details of species traits. Indeed, whereas the sign of diversity-stability relationships can depend, amongst other things, on the way interactions change with diversity, the described contributions to variability of species abundances classes reflect a generic outcome of the assembly of disordered systems. As illustrated in Fig. 5 and detailed in Appendix G, the sole requirement isthat interactions

34

~~in a species-rich community are sufficiently strong and heterogeneous.~~ relationships. It would be interesting to test whether this observation holds more generally, e.g., if it can explain the contrasting relationships recently reported by Pennekamp et al. (2018).

~~Our results showcase the fact that variability strongly depends on factors external to the system of interest. There are cases, however, in which this does not constitute a fundamental problem.When approaching a regime shift, early warning signals based on variability are generically independent of the perturbation or of the way that the response is observed (Scheffer et al., 2009)~~The type of perturbations affects which species abundance class contributes most to variability. In turn, the physical size of the system considered affects which perturbation type dominates. This is ~~because when a system approaches a global instability, most perturbations will excite the unstable direction, and most observation will detect it. Similarly, all stability measures should coincide near a catastrophic transition. In the absence or far from such transitions, stability metrics can branch out, as well as possible invariability measurements, and it is in this context that our work ought to be most relevant.~~ well known in population dynamics (Engen et al., 2008), but it also transposes to the community level. At small spatial scales, implying small populations, we may expect variability to be driven by demographic stochasticity. At larger scales, implying larger populations, demographic stochasticity will be negligible compared with environmental perturbations. Just as changing the perturbation type transforms the respective roles of common and rare species, patterns of variability at different scales should reflect different aspects of a community (Chalcraft, 2013), associated to different species abundance classes (abundant species at large spatial scales, rare/rarer species at small spatial scales).

Empirically determining the perturbation type, which is a preliminary step to test the stability patterns predicted in this paper, is a non-trivial task. To develop suitable methods, it might be helpful to first understand the link between the variability-abundance patterns (see

Figs. 4 and 5) and Taylor's (1961) law. The latter is an empirically accessible pattern, relating the mean and variance of population sizes. A close connection is indeed expected: we studied the behavior of the community response to an individual species perturbation, while Taylor's law focuses on the individual species response to a perturbation of the whole community. This duality also suggests that Taylor's law is, at the community level, strongly affected by species interactions. Although this is known (Kilpatrick and Ives, 2003), our approach could shed new light on the information regarding species interactions and other dynamical traits, actually contained in community-level Taylor's laws.

~~Theoretical consequences~~Link with other stability measures

We ~~could relate variability to~~ noted a connection between variability and asymptotic resilience, ~~the most commonly used stability metric~~ which is a popular notion in theoretical studies (Donohue et al., 2016). We ~~found~~ showed that asymptotic resilience is comparable to the largest variability in response to an immigration-type perturbation, which is often a perturbation of the rarest species (first panel of Fig. 4). While ~~the asymptotic rate of return to equilibrium~~ asymptotic resilience is sometimes considered as a measure representative of ~~the~~ collective recovery dynamics, we ~~recently showed~~ previously explained why that this is seldom the case (Arnoldi et al., 2018). The asymptotic rate of return ~~often reflects dynamical to equilibrium generally reflects~~ properties of rare "satellite" species, pushed at the edge of local extinction by abundant "core" species. ~~By contrast~~On the other hand, short-time return rates can exhibit qualitatively different properties related to more abundant species. ~~This suggest that~~

In fact, the multiple dimensions of variability are related to the multiple dimensions of return times. ~~Indeed, variability reflects~~Variability is an integral measure of the transient regime

36

following pulse perturbations, i.e., a superposition of responses to ~~pulse perturbations~~various pulses, some of which have just occurred and are thus hardly absorbed, while others occurred long ago and are ~~thus~~ largely resorbed. ~~Variability is thus an integral measure of the transient regime following pulse perturbations.~~ If abundant species are faster than rare ones (~~which, as we showed, is typically~~ the case in complex communities, see Appendix G), if they are also more strongly perturbed (e.g., by environmental perturbations), the bulk of the transient regime will be ~~relatively short. Thus~~ short: variability in response to environmental perturbations is associated with a short-term recovery~~dynamics~~. By contrast, if all species are, on average, equally displaced by perturbations (e.g., by immigration-type perturbations), rare species initially contribute to the overall community displacement as much as ~~abundant ones, and if they are much slower to recover (which is often the case), the bulk of the~~ do abundant ones. Since their recovery is typically very slow, the transient regime will be ~~longer. Thus~~ long: variability in response to immigration-type perturbations is associated with ~~the~~ a long-term ~~return rate to equilibrium (which converges towards asymptotic resilience)~~recovery.

~~The link between asymptotic resilience, immigration invariability and rare species, also suggests a connection with the notion of *feasibility*: the probability, for a given set of species, that a coexistence equilibrium exist, where all species have a positive abundance (Roberts, 1974; Grilli et a~~

~~. Indeed, in an assembly context there is a continuum from common, to rare, to extinct. If feasibility drops then we can also expect that some species will be rare, and will drive asymptotic resilience and worst-case immigration invariability. In other words, we should expect these three notions (feasibility, asymptotic resilience, worst-case immigration invariability) to go hand in hand in the context of community assembly.~~

~~One could think that asymptotic resilience, and thus variability in response to~~ Ecologists have long acknowledged the multi-faceted nature of ecological stability (Pimm, 1984; Grimm and Wissel, 1 , but here we show that a single facet (variability) is in itself inherently multidimensional,

37

thus suggesting that links across facets can be subtle. Short-term return rates may be linked with environmental variability, but environmental variability may have nothing to do with immigration-type ~~perturbations, should also be closely linked to May's (1972) seminal article predicting a "complexity bound" beyond which most systems are unstable. Indeed, as in many theoretical works since then (e.g. Gross et al., 2009; Allesina and Tang, 2012), stability in May's work referred to the probability of a random community matrix to be stable, thus defining a linear dynamical system with positive asymptotic resilience. In our work, however, we did not rely on the probability of drawing a stable state: starting from a random pool of species, we let community assembly play out to reach an equilibrium, which is stable by construction. This nuance is in an important one (Bunin, 2017). Yet, Biroli et al. (2017) recently revealed a connection between May's work and community assembly, showing that May's bound applies to Lotka-Volterra systems, predicting the diversity limit beyond which the community is in a collective state of marginal stability, or chaos. The growing instability with diversity predicted by May, however, is not to be seen in the asymptotic resilience of assembled communities, but in properties of their per-capita interaction matrix, which is independent of species abundances (see Appendix G). Recall that we found abundances to play no significant role in the response to demographic perturbations (middle panel of Fig. 4). This is because, in disordered communities, demographic variability is also an intrinsic feature of the per-capita interaction matrix (Barbier et al., 2018). Thus the link between May's work and ours is likely to be found in patterns of demographic variability. Furthermore, because the work of Biroli et al. shows that May's bound signals a collective dynamical shift in complex communities, it also suggests that demographic perturbations probe the collective response of ecosystems.~~

~~Although these reasonings go beyond the scope of this article, they clearly showcase the potential of the variability spectrum framework to encompass previously disconnected~~

38

theoretical works on ecological stability.

Empirical consequences

Of the two statistics of the variability spectrum that we studied (i.e. mean- and worst-case variability) , only the mean-case scenario is empirically accessible. Ideally it could be reconstructed from multiple observations of a same community under different environmental conditions. However, depending on the question addressed, simpler protocols may be sufficient. For instance, in diversity-stability studies, observing many communities in the same environment (e.g. undergoing a unique perturbation regime) is a way to assess an average response, because the direct effect of a perturbation on the community its *direction* depends both on the perturbation itself , and on the way individuals from different species perceive it. Thus, sampling many communities also spans many perturbation directions.

On the other hand, the worst-case scenario corresponds to a theoretical prediction that is unlikely to be observed. The potentially strong discrepancy between mean- and worst-case scenarios implies that the variability spectrum of communities should be expected to be broad, so that differences around an average are not solely caused by observational errors but can reflect the inherent multidimensionality of an ecosystem's response to perturbations.

Variability offers a convenient way to address the stability of ecosystems at different levels of organization. For instance, the coefficient of variation (CV) of total biomass has been used as a measure of stability at the ecosystem level (Tilman et al., 2006; Hector et al., 2010) . On the other hand, the weighted average CV of species biomass is typically interpreted as population-level stability. These two variability notions thus differ in the variables observed. By contrast, our approach was to consider, for a given observation scheme, the various responses caused by various types of perturbation. Empirical studies have reported a general

39

tendency for diversity to correlate positively with stability at the ecosystem level, but negatively at the population level (Jiang and Pu, 2009; Campbell et al., 2011). In Appendix I, with the same model communities used to generate Fig. 6, we corroborate these empirical findings. Instead of defining variability as mean variance, we considered CV-based stability measures, and indeed found ecosystem-level invariability to increase with diversity for all perturbation types, while population-level invariability always decreases (Fig. I1). This can be explained from the fact that, by construction, ecosystem-level stability gives a predominant weight to abundant species, while population-level stability gives a large weight to variability, the latter possibly related with long-term return rates and driven by rare species. Here, underlying the contrasting diversity-stability relationships, is again a contrasting role given to species depending on their abundance, but the difference is now due to the choice of observation itself instead of the perturbation type. This highlights the fact that the role given to species abundance classes, either because of inherent dynamical reasons or due to the choice of observation variable, is a fundamental driver of observed stability patterns.

While it is clear that the choice of observation predetermines the level of organization of interest, that the type of perturbations can also reflect the dynamical properties of distinct species abundance classes is a novel statement that opens the door to empirical investigations. For instance, the physical size of the system considered should affect which perturbation type predominates and thus which species abundance class is most likely to contribute to variability. Suppose that a spatially homogeneous community, say the predator-prey system considered in Fig. 3, is observed at two spatial scales. At the small scale, implying small populations, we can expect variability to be mostly caused by demographic stochasticity. At larger scales, implying larger populations, demographic stochasticity will be negligible compared with environmental perturbations. Just as changing the perturbation type transformed the variability spectra in our simple example presented in Fig. 3, patterns of variability at these two scales will

40

reflect different aspects of the community. Thus, without invoking spatial heterogeneity, there are reasons to expect a non-trivial spatial scaling of stability (Chalcraft, 2013), reflecting an underlying transition of the Because measures can be determined by different species abundance classes that contribute to the ecosystem's dynamical response to the perturbations that it faces. , we should not expect a general and simple connection to hold between facets of ecological stability.

Empirical testing of these ideas would require determining the type of perturbations affecting a given community. This means estimating the exponent α that characterizes the various perturbation types. This could be done, e.g. by identifying perturbation events and fitting a power-law to their effect on species as a function of the latter's abundance. One could also look for a direct relationship between the exponent α and that of Taylor's (1961) law that links mean and variance of population sizes. In fact Taylor's law is an output of our framework with perturbation type as an input, and thus, ought to affected by species interactions (Kilpatrick and Ives, 2003). It would thus be useful to check whether the simple models of the diversity-stability relationships based on an assumed Taylor's law are consistent with the predictions of our framework.

Conclusion

The multidimensional nature of variability can lead to conflicting predictions but, once acknowledged, but once this multidimensionality is acknowledged, it can be used to extensively probe the dynamical properties of different species abundance classes within a community, in a similar way as various diversity measures reflect the presence of different abundance classes. By shifting the focus from a single measure of variability to the variability spectrum, we could more clearly appreciate the dynamical richness of complex systems and demonstrate the impossibility of

41

~~any one-dimensional characterization of their stability. This applies beyond the technical setting of our work: although we did not consider strong non-linearities, autocorrelation of perturbations or spatial processes, these additional dimensions can also be used to probe and reveal other important dynamical behaviors (Zelnik et al., 2019). Overall, this work provides a dialectical perspective~~ community. In particular, in species-rich systems, we revealed a generic pattern emerging from ecological assembly, relating species abundance to their variability contribution. This allowed connections to be drawn between variability and statistics of abundance distributions. We argued that similar patterns should underlie ecosystem responses to other families of perturbations (e.g., pulse perturbations). Therefore, we conclude that embracing the whole set of a ecosystem responses can help provide a unifying view on ecological stability ~~. A community is not a mere aggregation of rare and abundant species, as these species can be rare and abundant as a product of their interactions with the rest of the community. Variability can probe the dynamics at the species level (rare to abundant species) but also of more collective properties. All are intertwined, and all contribute to a community's dynamical identity~~and shed new light on the meaning of empirical and theoretical stability patterns.

Acknowledgements

Literature Cited

Allesina, S., and S. Tang. 2012. Stability criteria for complex ecosystems. Nature 483:205–208.

Arnold, L. 1974. Stochastic Differential Equations: Theory and Applications. Dover Publications.

Arnoldi, J.-F., A. Bideault, M. Loreau, and B. Haegeman. 2018. How ecosystems recover from pulse perturbations: A theory of short- to long-term responses. Journal of Theoretical Biology 436:79–92.

Arnoldi, J.-F., and B. Haegeman. 2016. Unifying dynamical and structural stability of equilibria. Proceedings of the Royal Society of London A: Mathematical, Physical and Engineering Sciences 472:20150874.

Arnoldi, J.-F., B. Haegeman, T. Revilla, and M. Loreau. 2016a. Particularity of universal resilience patterns in complex networks. bioRxiv 056218.

Arnoldi, J.-F., M. Loreau, and B. Haegeman. 2016b. Resilience, reactivity and variability: A mathematical comparison of ecological stability measures. Journal of Theoretical Biology 389:47–59.

Barbier, M., J.-F. Arnoldi, G. Bunin, and M. Loreau. 2018. Generic assembly patterns in large ecological communities. Proceedings of the National Academy of Sciences 115:2156–2161.

Biroli, G., G. Bunin, and C. Cammarota. 2017. Marginally stable equilibria in critical ecosystems. arXiv 1710.03606.

Bunin, G. 2017. Ecological communities with Lotka-Volterra dynamics. Physical Review E 95:042414.

Campbell, V., G. Murphy, and T. N. Romanuk. 2011. Experimental design and the outcome and interpretation of diversity-stability relations. Oikos 120:399–408.

Chalcraft, D. R. 2013. Changes in ecological stability across realistic biodiversity gradients depend on spatial scale. Global Ecology and Biogeography 22:19–28.

Donohue, I., H. Hillebrand, J. M. Montoya, O. L. Petchey, S. L. Pimm, M. S. Fowler, K. Healy, A. L. Jackson, M. Lurgi, D. McClean, N. E. O'Connor, E. J. O'Gorman, and Q. Yang. 2016. Navigating the complexity of ecological stability. Ecology Letters 19:1172–1185.

Elton, C. 1946. Competition and the structure of ecological communities. Journal of Animal Ecology 15:54–68.

Engen, S., R. Lande, and B.-E. Saether. 2008. A general model for analysing Taylor's spatial scaling laws. Ecology 89:2612–2622.

Fowler, M. S., and L. Ruokolainen. 2013. Colonization, covariance and colour: Environmental and ecological drivers of diversity–stability relationships. Journal of theoretical biology 324:32–41.

Griffin, J. N., E. J. O'Gorman, M. C. Emmerson, S. R. Jenkins, A.-M. Klein, M. Loreau, and A. Symstad. 2009. Biodiversity and the stability of ecosystem functioning. Oxford University Press.

Grilli, J., M. Adorisio, S. Suweis, G. Barabás, J. R. Banavar, S. Allesina, and A. Maritan. 2017. Feasibility and coexistence of large ecological communities. Nature Communications 8:14389.

Grimm, V., and C. Wissel. 1997. Babel, or the ecological stability discussions: An inventory and analysis of terminology and a guide for avoiding confusion. Oecologia 109:323–334.

Gross, K., B. J. Cardinale, J. W. Fox, A. Gonzalez, M. Loreau, H. Wayne Polley, P. B. Reich, and J. van Ruijven. 2014. Species richness and the temporal stability of biomass production: A new analysis of recent biodiversity experiments. The American Naturalist 183:1–12.

Gross, T., L. Rudolf, S. A. Levin, and U. Dieckmann. 2009. Generalized models reveal stabilizing factors in food webs. Science 325:747–750.

Gurney, W., and R. M. Nisbet. 1998. Ecological Dynamics. Oxford University Press.

Haegeman, B., J.-F. Arnoldi, S. Wang, C. de Mazancourt, J. M. Montoya, and M. Loreau. 2016. Resilience, invariability, and ecological stability across levels of organization. bioRxiv 085852.

Haegeman, B., and M. Loreau. 2011. A mathematical synthesis of niche and neutral theories in community ecology. Journal of Theoretical Biology 269:150–165.

Hector, A., Y. Hautier, P. Saner, L. Wacker, R. Bagchi, J. Joshi, M. Scherer-Lorenzen, E. M. Spehn, E. Bazeley-White, M. Weilenmann, M. C. Caldeira, P. G. Dimitrakopoulos, J. A. Finn, K. Huss-Danell, A. Jumpponen, C. P. H. Mulder, C. Palmborg, J. S. Pereira, A. S. D. Siamantziouras, A. C. Terry, A. Y. Troumbis, B. Schmid, and M. Loreau. 2010. General stabilizing effects of plant diversity on grassland productivity through population asynchrony and overyielding. Ecology 91:2213–2220.

Hill, M. O. 1973. Diversity and evenness: A unifying notation and its consequences. Ecology 54:427–432.

Ives, A. R., and S. R. Carpenter. 2007. Stability and diversity of ecosystems. Science 317:58–62.

Ives, A. R., B. Dennis, K. L. Cottingham, and S. R. Carpenter. 2003. Estimating community stability and ecological interactions from time-series data. Ecological Monographs 73:301–330.

Jiang, L., and Z. Pu. 2009. Different effects of species diversity on temporal stability in single trophic and multitrophic communities. The American Naturalist 174:651–659.

Kilpatrick, A. M., and A. R. Ives. 2003. Species interactions can explain Taylor's power law for ecological time series. Nature 422:65–68.

Lande, R., S. Engen, and B.-E. Saether. 2003. Stochastic Population Dynamics in Ecology and Conservation. Oxford University Press.

Loreau, M., and C. de Mazancourt. 2013. Biodiversity and ecosystem stability: A synthesis of underlying mechanisms. Ecology Letters 16:106–115.

MacArthur, R. 1955. Fluctuations of animal populations and a measure of community stability. Ecology 36:533–536.

May, R. M. 1972. Will a large complex system be stable? Nature 238:413–414.

———. 1973a. Stability and Complexity in Model Ecosystems. Princeton University Press.

———. 1973b. Stability in randomly fluctuating versus deterministic environments. The American Naturalist 107:621–650.

McCann, K. S. 2000. The diversity-stability debate. Nature 405:228–233.

Pennekamp, F., M. Pontarp, A. Tabi, F. Altermatt, R. Alther, Y. Choffat, E. A. Fronhofer, P. Ganesanandamoorthy, A. Garnier, J. I. Griffiths, S. Greene, K. Horgan, T. M. Massie, E. Mächler, G. M. Palamara, M. Seymour, and O. L. Petchey. 2018. Biodiversity increases and decreases ecosystem stability. Nature 563:109–112.

Pimm, S. L. 1984. The complexity and stability of ecosystems. Nature 307:321–326.

———. 1991. The Balance of Nature? Ecological Issues in the Conservation of Species and Communities. University of Chicago Press.

Ripa, J., and A. R. Ives. 2003. Food web dynamics in correlated and autocorrelated environments. Theoretical Population Biology 64:369–384.

Roberts, A. 1974. The stability of a feasible random ecosystem. Nature 251:607–608.

Ruokolainen, L., and M. S. Fowler. 2008. Community extinction patterns in coloured environments. Proceedings of the Royal Society of London B: Biological Sciences 275:1775–1783.

Ruokolainen, L., A. Linden, V. Kaitala, and M. S. Fowler. 2009. Ecological and evolutionary dynamics under coloured environmental variation. Trends in Ecology & Evolution 24:555–563.

Scheffer, M., J. Bascompte, W. A. Brock, V. Brovkin, S. R. Carpenter, V. Dakos, H. Held, E. H. van Nes, M. Rietkerk, and G. Sugihara. 2009. Early-warning signals for critical transitions. Nature 461:53–59.

Taylor, L. R. 1961. Aggregation, variance and the mean. Nature 189:732–735.

Tilman, D. 1996. Biodiversity: Population versus ecosystem stability. Ecology 77:350–363.

Tilman, D., P. B. Reich, and J. M. H. Knops. 2006. Biodiversity and ecosystem stability in a decade-long grassland experiment. Nature 441:629–632.

Tilman, D., D. Wedin, and J. Knops. 1996. Productivity and sustainability influenced by biodiversity in grassland ecosystems. Nature 379:718–720.

Turelli, M. 1977. Random environments and stochastic calculus. Theoretical Population Biology 12:140–178.

Van Kampen, N. G. 1997. Stochastic Processes in Physics and Chemistry. Elsevier.

Vasseur, D. A., and P. Yodzis. 2004. The color of environmental noise. Ecology 85:1146–1152.

Wang, S., and M. Loreau. 2014. Ecosystem stability in space: α, β and γ variability. Ecology Letters 17:891–901.

Wang, S., M. Loreau, J.-F. Arnoldi, J. Fang, K. A. Rahman, S. Tao, and C. de Mazancourt. 2017. An invariability-area relationship sheds new light on the spatial scaling of ecological stability. Nature Communications 8:15211.

Yachi, S., and M. Loreau. 1999. Biodiversity and ecosystem productivity in a fluctuating environment: The insurance hypothesis. Proceedings of the National Academy of Sciences 96:1463–1468.

Zelnik, Y. R., J.-F. Arnoldi, and M. Loreau. 2019. The three regimes of spatial recovery. Ecology 100:e02586.

Appendices

The Appendices are organized as follows: Appendix A through D provides a self-contained presentation of the mathematical foundations of our variability theory. Appendix E through H provide details concerning specific applications considered in the main text: two-species communities in Appendix E, complex Lotka-Volterra communities in appendices F and G, and the link between abundance statistics and variability in Appendix H. A list of the most important notation used in the Appendices is given in Table A1.

A   Response to white-noise perturbation

We describe the response of a linear dynamical system, representing the dynamics of displacement of species around an equilibrium value, to a white-noise perturbation. Stochastic perturbations in continuous time are mathematically quite subtle (see, e.g., Turelli, 1977). However, in the setting of linear dynamical systems, the effect of a white-noise perturbation can be analyzed relatively easily. Because this analysis is not readily available in the ecology literature, we present here a short overview. We start from a fomulation in vector notation,

$$\frac{d\boldsymbol{x}}{dt} = A\boldsymbol{x} + \boldsymbol{\xi}(t), \tag{A1}$$

where $\boldsymbol{x} = (x_i)$ denotes the vector of species displacements, $\boldsymbol{\xi} = (\xi_i)$ the vector of species perturbations, and $A = (A_{ij})$ the community matrix.

Suppose that the perturbation $\boldsymbol{\xi}(t)$ consists in a sequence of pulses. We denote the times at which these pulses occur by t_k, and the corresponding pulse directions by $\boldsymbol{u}_k = (u_{k,i})$. The

Table A1: Most important notation used throughout the Appendices

symbol	meaning	equation
σ_{in}^2	per species variance of applied perturbation	(B2)
σ_{out}^2	per species variance of system response to perturbation	(B4, D3)
C_u	covariance matrix of individual pulses in multi-pulse perturbation	(A3)
f	frequency at which pulses occur in multi-pulse perturbation	
E	perturbation direction, proportional to fC_u	(B5)
C_x	covariance matrix of species responses to perturbation	(A5, A9)
$\mathcal{L}$	solution of Lyapunov equation, used to compute stationary C_x	(A7, A8)
$\mathcal{V}_\alpha$	variability for perturbation type α; when index α is omitted, immigration-type perturbations are assumed ($\alpha = 0$)	(D4)
$\mathcal{V}^{\text{worst}}$	mean-case variability, i.e., variability averaged over perturbation directions	(C2, D5)
$\mathcal{V}^{\text{mean}}$	worst-case variability, i.e., variability maximized over perturbation directions	(C3, D6)
$\mathcal{V}^{\text{spec } i}$	variability for the perturbation that affects only species i	
$\mathcal{I}$	invariability, i.e., variability-based stability measure	(B6)

multi-pulse perturbation can then be written as

$$\boldsymbol{\xi}(t) = \sum_k \delta(t - t_k)\, \boldsymbol{u}_k. \tag{A2}$$

where we have used the Dirac delta function $\delta(t)$.

We model both the pulse times t_k and the pulse directions $\boldsymbol{u}_k$ as random variables. Specifically, we assume that the pulse times are distributed according to a Poisson point process with intensity f. This means that the probability that a pulse occurs in a small time interval of length Δs is equal to $f\Delta s$, and that this occurrence is independent of any other model randomness. We denote the average over the pulse times t_k by $\mathbb{E}_f$.

Furthermore, we assume that the pulse directions $\boldsymbol{u}_k$ are independent (mutually independent, and independent of any other model randomness) and identically distributed. They have zero mean, and their second moments are given by the covariance matrix C_u. That is, denoting the average over the pulse directions $\boldsymbol{u}_k$ by $\mathbb{E}_u$, we have $\mathbb{E}_u\, u_{k,i} = 0$, $\mathbb{E}_u\, u_{k,i}^2 = C_{u,ii}$, $\mathbb{E}_u\, u_{k,i}u_{k,j} = C_{u,ij}$, and $\mathbb{E}_u\, u_{k,i}u_{\ell,i} = \mathbb{E}_u\, u_{k,i}u_{\ell,j} = 0$ for $i \neq j$ and $k \neq \ell$. The latter equations can be written in vector notation,

$$C_u = \mathbb{E}_u\, \boldsymbol{u}_k \boldsymbol{u}_k^\top \qquad \text{and} \qquad \mathbb{E}_u\, \boldsymbol{u}_k \boldsymbol{u}_\ell^\top = 0. \tag{A3}$$

We use this information to compute the statistics of species displacements $\boldsymbol{x}(t)$. Because the system response to a single pulse perturbation at time t_k in directon $\boldsymbol{u}_k$ is equal to $e^{(t-t_k)A}\boldsymbol{u}_k$, the system response to the sequence (A2) of pulse perturbations is equal to

$$\boldsymbol{x}(t) = \sum_{k|t_k < t} e^{(t-t_k)A}\, \boldsymbol{u}_k. \tag{A4}$$

51

Taking the mean over the perturbation directions, we obtain

$$\mathbb{E}_u \, \boldsymbol{x}(t) = \sum_{k|t_k<t} e^{(t-t_k)A} \, \mathbb{E}_u \, \boldsymbol{u}_k = 0,$$

showing that the species displacements fluctuate around the unperturbed equilibrium.

Next, we compute the covariance matrix of the species displacements,

$$C_x = \mathbb{E}_{f,u} \, \boldsymbol{x}(t)\boldsymbol{x}(t)^\top. \tag{A5}$$

We substitute the response to the multi-pulse perturbation, ~~equation~~ eq. (A4),

$$C_x = \mathbb{E}_{f,u} \sum_{k|t_k<t} e^{(t-t_k)A} \, \boldsymbol{u}_k \sum_{\ell|t_\ell<t} \boldsymbol{u}_\ell^\top \, e^{(t-t_\ell)A^\top}$$

$$= \mathbb{E}_f \sum_{k|t_k<t \, \ell|t_\ell<t} e^{(t-t_k)A} \, \mathbb{E}_u \, \boldsymbol{u}_k\boldsymbol{u}_\ell^\top \, e^{(t-t_\ell)A^\top}$$

$$= \mathbb{E}_f \sum_{k|t_k<t} e^{(t-t_k)A} \, \mathbb{E}_u \, \boldsymbol{u}_k\boldsymbol{u}_k^\top \, e^{(t-t_k)A^\top}$$

$$= \mathbb{E}_f \sum_{k|t_k<t} e^{(t-t_k)A} \, C_u \, e^{(t-t_k)A^\top},$$

where we have used ~~equation~~ eq. (A3). To take the average over the pulse times, we partition the time axis in small intervals of length Δs. Writing $s_n = n\Delta s$ for any integer n, we get

$$C_x = \sum_{n|s_n<t} e^{(t-s_n)A} \, C_u \, e^{(t-s_n)A^\top} f\Delta s,$$

because the contribution of term n is equal to $e^{(t-s_n)A} \, C_u \, e^{(t-s_n)A^\top}$ with probability $f\Delta s$, and

52

zero otherwise. Assuming that the time intervals Δs are infinitesimal, we find the integral

$$
\begin{aligned}
C_x &= \int_{-\infty}^{t} e^{(t-s)A} C_u e^{(t-s)A^\top} f ds \\
&= \int_{0}^{\infty} e^{sA} C_u e^{sA^\top} f ds \\
&= \int_{0}^{\infty} e^{sA} \left(f C_u \right) e^{sA^\top} ds.
\end{aligned} \tag{A6}
$$

Hence, we have obtained the stationary covariance matrix of the species displacements under a stochastic multi-pulse perturbation.

A white-noise perturbation corresponds to a special case of the stochastic multi-pulse perturbation, namely, to the case of extremely frequent pulses (large f) of extremely small size (small $\|\boldsymbol{u}\|$). More precisely, we have to take the coupled limit $f \to \infty$ and $C_u \to 0$ while keeping $f C_u$ constant. Because equation eq. (A6) depends on f and C_u through the product $f C_u$ only, the same expression is also valid for white-noise perturbations.

Alternatively, the stationary covariance matrix C_x can be obtained by solving the so-called Lyapunov equation,

$$
AC + CA^\top + E = 0, \tag{A7}
$$

where E is the covariance matrix characterizing the white noise, equal to $f C_u$ in our case. Indeed, it can be verified that equation eq. (A6) satisfies equation eq. (A7),

$$
\begin{aligned}
AC_x + C_x A^\top &= \int_{0}^{\infty} \left(A e^{sA} f C_u e^{sA^\top} ds + e^{sA} f C_u e^{sA^\top} A^\top \right) ds \\
&= \int_{0}^{\infty} \frac{d}{ds} \left(e^{sA} f C_u e^{sA^\top} \right) ds \\
&= e^{sA} f C_u e^{sA^\top} \Big|_{s \to \infty} - e^{sA} f C_u e^{sA^\top} \Big|_{s=0} \\
&= -f C_u.
\end{aligned}
$$

For a stable matrix A this is the unique solution of the Lyapunov equation, for which we introduce the short-hand notation $\mathcal{L}(A, E)$,

$$\mathcal{L}(A, E) = \int_0^\infty e^{sA} E \, e^{sA^\top} ds. \tag{A8}$$

Hence, we can write

$$C_x = \mathcal{L}(A, fC_u), . \tag{A9}$$

~~which is the notation used in the main text.~~ From a numerical viewpoint, the covariance matrix C_x can be easily obtained by solving the Lyapunov ~~equation~~ eq. (A7), which can be written as a system of S^2 linear equations, rather than by computing the integral in (A8). Note also that solution of Lyapunov equation is linear in the perturbation covariance matrix,

$$\mathcal{L}(A, c_1 E_1 + c_2 E_2) = c_1 \, \mathcal{L}(A, E_1) + c_2 \, \mathcal{L}(A, E_2). \tag{A10}$$

B   Construction of variability measure

We explain the construction of the variability measure ~~$\mathcal{V}(E)$.~~ $\mathcal{V}$, see eq. (4) in the main text. The construction is based on the comparison of the intensity of the system response relative to the intensity of the applied perturbation. It should be stressed that, while we take special care of quantifying these intensities in a reasonable way, alternative choices are possible.

Perturbation intensity   A reasonable measure of the perturbation intensity should increase with the number of pulses and the intensity of each pulse separately. In particular, we expect it to be proportional to the pulse frequency f and to some function of the pulse covariance matrix C_u.

We propose to look at the squared displacements $\|\boldsymbol{u}_k\|^2$ induced by pulses $\boldsymbol{u}_k$. The accumulated squared displacement in time interval $[t, t+T]$ is

$$\sum_{t_k \in [t,t+T]} \|\boldsymbol{u_k}\|^2.$$

Taking the average over pulse times and pulse directions,

$$\mathbb{E}_{f,u} \sum_{t_k \in [t,t+T]} \|\boldsymbol{u_k}\|^2 = \sum_{n | t < s_n < t+T} \mathbb{E}_u \|\boldsymbol{u}\|^2 f \Delta s,$$

where we have partitioned the time axis in small intervals of length Δs (see derivation of ~~equation~~eq. (A6)). Then,

$$\mathbb{E}_{f,u} \sum_{t_k \in [t,t+T]} \|\boldsymbol{u_k}\|^2 = \mathrm{Tr}(C_u) f T.$$

The result is proportional to the length T of the considered time interval. The average accumulated squared displacement per unit of time is

$$\frac{1}{T} \mathbb{E}_{f,u} \sum_{t_k \in [t,t+T]} \|\boldsymbol{u_k}\|^2 = \mathrm{Tr}(f C_u). \tag{B1}$$

As expected, this quantity is proportional to the pulse frequency f and increases with the pulse covariance matrix C_u. Note also that f and C_u appear as a product, so that the expression is compatible with the white-noise limit.

~~Equation~~Eq. (B1) quantifies the intensity of the perturbation applied to the entire ecosystem. This measure is not directly appropriate to normalize the pertubation intensity across systems. Indeed, when keeping the total perturbation intensity constant, the perturbation applied to a given species would be weaker in a community with a larger number of species. To eliminate this artefact, we normalize the perturbation intensity on a per species basis.

Thus, we propose to quantify the perturbation intensity as

$$\sigma_{\text{in}}^2 = \frac{f}{S} \operatorname{Tr} C_u. \tag{B2}$$

Response intensity   We measure the intensity of the system response in terms of the co-variance matrix C_x. This matrix encodes the statistical properties of the ~~biomass~~ abundance (or biomass) fluctuations in stationary state. For example, species ~~biomass~~ abundance $x_i(t)$ fluctuates around its equilibrium value N_i with variance $C_{x,ii}$. More generally, we can describe the fluctuations of any function φ of species ~~biomasses~~ abundance. The dynamics near equilibrium are

$$\varphi(\boldsymbol{n}(t)) = \varphi(\boldsymbol{N}) + \boldsymbol{v}^\top \boldsymbol{x}(t),$$

where vector $\boldsymbol{v} = \nabla\varphi$ is the gradient of the function φ evaluated at the equilibrium $\boldsymbol{N}$. This vector gives the direction in which the system fluctuations are observed. Then, denoting the temporal mean and variance by $\mathbb{E}_t$ and Var_t, we have

$$\begin{aligned}
\operatorname{Var}_t\left(\varphi(\boldsymbol{n}(t))\right) &= \mathbb{E}_t\left(\left(\boldsymbol{v}^\top \boldsymbol{x}(t)\right)^2\right) \\
&= \mathbb{E}_t\left(\boldsymbol{v}^\top \boldsymbol{x}(t)\boldsymbol{x}(t)^\top \boldsymbol{v}\right) \\
&= \boldsymbol{v}^\top \mathbb{E}_t\left(\boldsymbol{x}(t)\boldsymbol{x}(t)^\top\right)\boldsymbol{v} \\
&= \boldsymbol{v}^\top C_x\, \boldsymbol{v}. \tag{B3}
\end{aligned}$$

We use this variance to quantify the intensity of the system response. Rather than choosing a particular vector $\boldsymbol{v}$, we consider the average over all observation directions. Specifically, we restrict attention to unit vectors $\boldsymbol{v}$ and average over the uniform distribution of such vectors.

Denoting this average by $\mathbb{E}_v$, we get

$$\mathbb{E}_v \operatorname{Var}_t\big(\varphi(\boldsymbol{n}(t))\big) = \mathbb{E}_v \big(\boldsymbol{v}^\top C_x \boldsymbol{v}\big) = \operatorname{Tr} \mathbb{E}_v \boldsymbol{v}\boldsymbol{v}^\top C_x.$$

It follows from species symmetry that the average $\mathbb{E}_v \boldsymbol{v}\boldsymbol{v}^\top$ is proportional to the unit matrix. Moreover, because $\operatorname{Tr} \boldsymbol{v}\boldsymbol{v}^\top = 1$ for all vectors $\boldsymbol{v}$, the constant of proportionality is equal to $\frac{1}{S}$. Hence,

$$\mathbb{E}_v \operatorname{Var}_t\big(\varphi(\boldsymbol{n}(t))\big) = \frac{1}{S}\operatorname{Tr} C_x.$$

Therefore, we propose to quantify the response intensity as

$$\sigma_{\text{out}}^2 = \frac{1}{S}\operatorname{Tr} C_x. \tag{B4}$$

Variability and invariability We define variability $\mathcal{V}$ as the ratio of the response intensity σ_{out}^2 and the perturbation intensity σ_{in}^2,

$$\mathcal{V} = \frac{\sigma_{\text{out}}^2}{\sigma_{\text{in}}^2} = \frac{\frac{1}{S}\operatorname{Tr} C_x}{\frac{f}{S}\operatorname{Tr} C_u} = \frac{\operatorname{Tr} C_x}{f \operatorname{Tr} C_u}.$$

Substituting ~~equation~~ eq. (A9) for C_x, we get

$$\mathcal{V} = \frac{\operatorname{Tr} \mathcal{L}(A, fC_u)}{f \operatorname{Tr} C_u} = \operatorname{Tr} \mathcal{L}\big(A, \frac{C_u}{\operatorname{Tr} C_u}\big),$$

where we have used the linearity property (A10). We see that only the normalized perturbation covariance matrix matters in this expression. That is, the variability measure focuses on the directional effect of the perturbation. We make this dependence explicit in the notation, and write

$$\mathcal{V}(E) = \operatorname{Tr} \mathcal{L}(A, E), \tag{B5}$$

57

where $E = \frac{C_u}{\operatorname{Tr} C_u}$ is the perturbation direction, i.e., a covariance matrix with unit trace.

Variability is inversely related to stability: the more variable an ecosytem, the less stable it is. For purpose of comparison, we construct a stability measure based on variability $\mathcal{V}(E)$, which we call invariability $\mathcal{I}(E)$,

$$\mathcal{I}(E) = \frac{1}{2\,\mathcal{V}(E)}. \tag{B6}$$

The factor 2 in this definition guarantees that we recover asymptotic resilience for the simplest dynamical systems. To see this, consider a system of S non-interacting species, in which all species have the same return rate λ. The community matrix is equal to $A = -\lambda \mathbb{1}$ where $\mathbb{1}$ denotes the identity matrix. From the Lyapunov equation (A7) we get the stationary covariance matrix $\mathcal{L}(A, E) = \frac{1}{2\lambda}E$. Therefore, $\mathcal{V}(E) = \frac{1}{2\lambda}$ and $\mathcal{I}(E) = \lambda$, which is equal to the asymptotic resilience of this example system.

C   Worst-case and mean-case variability

Worst-case variability is defined as

$$\mathcal{V}^{\mathrm{worst}} = \max_{E} \mathcal{V}(E) = \max_{E} \operatorname{Tr} \mathcal{L}(A, E) \tag{C1}$$

where the maximum is taken over perturbation directions, i.e., over covariance matrices E with $\operatorname{Tr} E = 1$. The function $\operatorname{Tr} \mathcal{L}(A, E)$ is linear in the perturbation direction E, see ~~equation~~ eq. (A10), and the set of perturbation directions is convex. Hence, the maximum is reached at an extreme point, that is, on the boundary of the set. The extreme points are the purely directional perturbations (see Appendix E for the argument in the two-species case), so that the maximum is reached at a purely directional perturbation. Arnoldi et al. (2016b) showed that the worst-case variability can be easily computed, namely, as a specific norm of the

operator $\widehat{A}^{-1}$ that maps E to $\mathcal{L}(A, E)$. Concretely

$$\widehat{A} = A \otimes \mathbb{1} + \mathbb{1} \otimes A,$$

so that , defining $\widehat{A} = A \otimes \mathbb{1} + \mathbb{1} \otimes A$,

$$\mathcal{V}^{\text{worst}} = ||\widehat{A}^{-1}||, \tag{C2}$$

where $|| \cdot ||$ stands for the spectral norm of $S^2 \times S^2$ matrices.

To define **mean-case variability** $\mathcal{V}^{\text{mean}}$, we assume a probability distribution over the perturbation directions, and compute the mean system response over this distribution. Due to the linearity property (A10), this mean response is equal to the response to the mean perturbation direction. Hence, we do not have to specify the full probability distribution over the perturbation directions; it suffices to determine the mean perturbation direction. As can be directly verified in the two-species case (Appendix E), if, averaged over the distribution of perturbation directions, perturbation intensities are evenly distributed across species, and positive and negative correlations between species perturbations cancel out, then the mean perturbation direction is adirectional. This corresponds to the center of the set of perturbation directions (the disc center in the two-species case the disc center represented in Fig. 3), and is proportional to the identity matrix, that is, $E = \frac{1}{S}\mathbb{1}$. Therefore,

$$\mathcal{V}^{\text{mean}} = \text{Tr}\, \mathcal{L}(A, \tfrac{1}{S}\mathbb{1}). \tag{C3}$$

D Perturbation types and variability

The perturbation type (environmental-, demographic- or immigration-type) affects how the perturbation intensity is distributed across species. Therefore, it also affects our measure of variability, as defined in Appendix B. Here we describe how the variability definition has to be modified.

We defined variability measure (B5) as the intensity of the system response relative to the intensity of the applied perturbation. To quantify the perturbation intensity in the case of ~~biomass-dependent~~ abundance-dependent perturbations, we distinguish the intrinsic effect of the perturbation on a species, which does not depend on the species' ~~biomass~~abundance, and the total effect of the perturbation on the species, which does depend on ~~biomass~~abundance. We propose to express the perturbation intensity in terms of the intrinsic perturbation, while it is the total perturbation that acts on the species dynamics.

Formally, for species i, we denote the intrinsic perturbation by $\xi_i^{\text{intr}}(t)$ and the total perturbation by $\xi_i^{\text{tot}}(t)$. Then, for a type-α perturbation, we have

$$\xi_i^{\text{tot}}(t) = N_i^{\frac{\alpha}{2}}\,\xi_i^{\text{intr}}(t), \tag{D1}$$

where N_i is the ~~biomass~~ abundance of species i. Thus, the intrinsic perturbation $\xi^{\text{intr}}(t)$ can be interpreted as the ~~perturbation per unit of biomass. Equation~~ per capita perturbation strength. Eq. (D1) can be written in vector notation as

$$\boldsymbol{\xi}^{\text{tot}}(t) = D^{\frac{\alpha}{2}}\boldsymbol{\xi}^{\text{intr}}(t), \tag{D2}$$

where D is the diagonal matrix whose entries are species equilibrium ~~biomass~~ values ($D_{ii} = N_i$).

Both the intrinsic and total perturbation are multi-pulse. If we denote the pulses of the intrinsic perturbation by $\boldsymbol{u}_k$, then, by ~~equation~~eq. (D2), those of the total perturbation are ~~$D^\alpha \boldsymbol{u}_k$~~$D^{\frac{\alpha}{2}}\boldsymbol{u}_k$. Then, to quantify the perturbation intensity, we use the covariance matrix of the pulses in the intrinsic perturbation. ~~Repeating the~~ The derivation leading to ~~equation~~eq. (B2) ~~, we have~~

$$\sigma_{\text{in}}^2 = \frac{1}{S}\text{Tr}\big(f C_u\big).$$

is still valid. However, to compute the covariance matrix of the species displacements, we use the covariance matrix of the pulses in the total perturbation. This corresponds to replacing C_u by $D^{\frac{\alpha}{2}}C_u D^{\frac{\alpha}{2}}$ in the derivation of ~~equation~~eq. (B4), so that we get

$$\sigma_{\text{out}}^2 = \frac{1}{S}\text{Tr}\,\mathcal{L}\big(A, f D^{\frac{\alpha}{2}} C_u D^{\frac{\alpha}{2}}\big). \tag{D3}$$

The variability measure for a type-α perturbation becomes

$$\mathcal{V}_\alpha = \frac{\sigma_{\text{out}}^2}{\sigma_{\text{in}}^2} = \text{Tr}\,\mathcal{L}\big(A, \frac{D^{\frac{\alpha}{2}} C_u D^{\frac{\alpha}{2}}}{\text{Tr}\,C_u}\big),$$

or, in terms of the (intrinsic) perturbation direction E,

$$\mathcal{V}_\alpha(E) = \text{Tr}\,\mathcal{L}\big(A, D^{\frac{\alpha}{2}} E D^{\frac{\alpha}{2}}\big). \tag{D4}$$

Applying the same arguments as in Appendix C~~)~~, we find that worst-case variability,

$$\mathcal{V}_\alpha^{\text{worst}} = \max_E \mathcal{V}_\alpha(E) = \max_E \text{Tr}\,\mathcal{L}\big(A, D^{\frac{\alpha}{2}} E D^{\frac{\alpha}{2}}\big),$$

is attained at a perfectly correlated perturbation. If we define the operator (an $S^2 \times S^2$

matrix)

$$\mathcal{D}_\alpha = D^{\frac{\alpha}{2}} \otimes D^{\frac{\alpha}{2}},$$

then the worst case-variability can be computed as

$$\mathcal{V}_\alpha^{\text{worst}} = ||\widehat{A}^{-1} \circ \mathcal{D}_\alpha||, \tag{D5}$$

where $|| \cdot ||$ is the spectral norm for $S^2 \times S^2$ matrices. On the other hand, the mean-case variability,

$$\mathcal{V}_\alpha^{\text{mean}} = \text{Tr}\,\mathcal{L}\big(A, \tfrac{1}{S}D^\alpha\big), \tag{D6}$$

is attained by the uniform, uncorrelated perturbation.

E   Perturbation directions in two dimensions

Variability spectra are built on the notion of perturbation directions. They are characterized by a covariance matrix E with $\text{Tr}\,E = 1$. To gain some intuition, we study the set of perturbation directions in the case of two species.

Any perturbation direction E in two dimensions can be written as

$$E = \begin{pmatrix} 1 - x & y \\ y & x \end{pmatrix}. \tag{E1}$$

with $0 \leq x \leq 1$ and $y^2 \leq x(1 - x)$. The first inequality guarantees that the elements on the diagonal are variances, i.e., positive numbers. The second inequality guarantees that the off-diagonal element is a proper covariance, in particular, that the correlation coefficient is contained between -1 and 1. Note ~~also~~ that matrix (E1) has always $\text{Tr}\,E = 1$.

It follows from ~~equation~~ eq. (E1) that the set of perturbation directions in two dimensions is parameterized by two numbers x and y. Using these numbers as axes of a two-dimensional plot, we see that the set of perturbation directions corresponds to a disc with radius 0.5 and centered at $(0.5, 0)$ (~~cf.~~ see Fig. 3).

It is instructive to study the position of specific perturbation directions on the disc. The point $(0, 0)$ corresponds to a perturbation affecting only the first species, whereas point $(1, 0)$ is a perturbation only affecting the second species. More generally, any point on the boundary of the disc correspond to a multi-pulse perturbation for which the individual pulses have a fixed direction. For example, the point $(0.5, 0.5)$ is a perturbation for which each pulse has the same effect on species 1 and species 2, whereas the perturbation corresponding to point $(0.5, -0.5)$ consists of pulses that affect the two species equally strongly, but in an opposite way. Perturbations on the boundary are *perfectly correlated*.

The perturbations towards the center of the disc are composed of pulses with more variable directions. For example, a multi-pulse perturbation for which half of the pulses affect only the second species, and the other pulses affect the two species equally strongly corresponds to the point $\frac{1}{2}(0, 1) + \frac{1}{2}(0.5, 0.5) = (0.25, 0.75)$. The mixture of different pulse directions is the strongest at the center of the disc $(0.5, 0)$. Examples of ways to realize this perturbation are $\frac{1}{2}(0, 0) + \frac{1}{2}(1, 0)$, $\frac{1}{2}(0.5, 0.5) + \frac{1}{2}(0.5, -0.5)$ and $\frac{1}{4}(0, 0) + \frac{1}{4}(0.5, 0.5) + \frac{1}{4}(1, 0) + \frac{1}{4}(0.5, -0.5)$. In each of these example, the pulses have their intensities, averaged over time, evenly distributed across species, and affect them, again averaged over time, in an uncorrelated way. The perturbation corresponding to the point $(0.5, 0)$ is thus evenly distributed across species but uncorrelated in time.

F   Random Lotka-Volterra model

~~Consider~~ The communities used in Figs. 4, 5 and 6 are constructed from the Lotka-Volterra model with random parameters. We consider a pool of species ~~following random Lotka-Volterra interactions~~ governed by the dynamics

$$\frac{dN_i(t)}{dt} = \frac{r_i N_i(t)}{K_i}\left(K_i - N_i - \sum_{\substack{j=1 \\ j\neq i}}^{S_{\text{pool}}} B_{ij}N_j(t)\right), \tag{F1}$$

and we let the dynamics settle to an equilibrium community of S remaining species. ~~In the above equation, the fact that species j has an effect of species i is noted as $j \rightsquigarrow i$. We fixed the network connectance of $\frac{1}{2}$, so that species interact, on average, with half of the pool. By gradually increasing the size of the pool and drawing random parameters – growth~~ By drawing random values for the parameters – growth rates r_i, carrying capacities K_i, and ~~interaction strengths~~ competition coefficients B_{ij} – we ~~generated many different~~ generate communities of various diversity. ~~We consider a single trophic level, representing unstructured, mostly competitive, communities. The mean interaction strength is set to 0.1 and its standard deviation to 0.1, thus allowing some occasional~~

For the communities in Fig. 4, we set $S_{\text{pool}} = 50$, and chose the parameter values as follows,

r_i randomly drawn from $\mathcal{N}(1, 0.2)$, a normal distribution with mean 1 and standard deviation 0.2 (independent draws for different species)

K_i drawn from $\mathcal{N}(1, 0.2)$

B_{ij} half of the competition coefficients are set equal to 0; the other half are drawn from $\mathcal{N}(0.1, 0.1)$.

This procedure resulted in a community of $S = 50$ persistent species. Note that some of the competition coefficients can be negative, so that there can be positive interactions (e.g. facilitation). ~~Growth rates~~

For the communities in the top row of Fig. 5, we followed the same procedure, except that we changed the way of generating the competition coefficients B_{ij}. In the case without interactions, all B_{ij} were set zero; in the case with weak interactions, the non-zero coefficients B_{ij} were drawn from $\mathcal{N}(0.02, 0.02)$; and in the case with strong interactions, the non-zero B_{ij} were drawn from $\mathcal{N}(0.1, 0.1)$, as for the community of Fig. 4.

We applied a similar procedure to obtain the bottom row of Fig. 5, but for these communities the growth rates r_i and carrying capacities ~~are independently drawn~~ K_i were not drawn independently. Instead, we first drew auxiliary variables a_i from $\mathcal{N}(1, 0.2)$, b_i from ~~a normal distribution of unit mean and 0.2 standard deviation~~ $\mathcal{N}(1, 0.1)$ and c_i from $\mathcal{N}(1, 0.1)$, and then set $r_i = b_i a_i$ and $K_i = c_i / a_i$.

~~Increasing the~~ For the communities of Fig. 6, we varied the size of the ~~pool from one species~~ species pool S_{pool} so that the realized species richness covered the range from 1 to 20. Specifically, we drew S_{pool} randomly from 1 to ~~one hundred we generated communities of various realized diversity. We repeated the process until we had 50~~ 100, and generated the parameter values as in Fig. 4. We repeated this procedure many times, until obtaining 1000 communities for each value of realized ~~diversity, from 1 to 30. For each realization of the random~~ species richness S from 1 to 20. Then, for each realized community, and ~~a given perturbation type we then~~ for each of the three perturbation types ($\alpha = 0$, $\alpha = 1$ and $\alpha = 2$), we generated 1000 random perturbations leading to a variability distribution of 1000 values ~~of variability. From each variability distribution we extracted its mean, its first and second quartile, its maximum and minimum values. From the~~. From the variability distributions we extracted median, 5th and 95th percentile, and minimum and maximum. For

the realized communities we computed asymptotic resilience, worst-case variability and the prediction for the median. Finally, we computed the median of these statistics and predictions, all represented in Fig. 6.

G Genericity in strongly interacting communities

We give some elements as to why the behavior reported in Figs. 4 and 5 in the main text can be expected to be a general trend in diverse communities of interacting species. Denote by $\mathcal{V}_\alpha^{\mathrm{spec}\,i}$ the community variability induced by a type-α perturbation that is fully focused on a single species i. We are interested in the relationship between this variability and the equilibrium abundance N_i of the perturbed species i.

First, note that for single-species perturbations the variability metrics $\mathcal{V}_\alpha^{\mathrm{spec}\,i}$ for different perturbation types α are directly linked. From definition (D4) we get that

$$\mathcal{V}_\alpha^{\mathrm{spec}\,i} = N_i^\alpha\, \mathcal{V}_{\alpha=0}^{\mathrm{spec}\,i}. \tag{G1}$$

Hence, it suffices to study the behavior of $\mathcal{V}_{\alpha=0}^{\mathrm{spec}\,i}$.

Next, consider again the Lotka-Volterra dynamics (F1) from the perspective of a focal species i. If a stable equilibrium exists in which the focal species survives, small displacements from equilibrium $x_i = N_i(t) - N_i$ are met with

the dynamics

$$\frac{dx_i}{dt} = \frac{r_i N_i}{K_i}\left(-x_i - \sum_{j \neq i} B_{ij} x_j\right) = \frac{1}{\tau_i}\left(-x_i - \sum_{j \neq i} B_{ij} x_j\right), \tag{G2}$$

~~In this expression τ_0 sets the~~ where $\tau_i = \frac{K_i}{r_i N_i}$ has units of time. We claim that τ_i sets a characteristic time scale of the focal species dynamics. ~~This species-specific time scale~~; it measures the typical time it takes for the species to recover from a perturbation that displaces it from its equilibrium. This species response time is directly related to the species' ~~contribution to variability. Indeed,~~ variability $\mathcal{V}_{\alpha=0}^{\text{spec } i}$: the slower the species, the larger the impact of a repeated perturbation acting on this species, and the larger the ~~species' contribution to variability~~ induced variability.

We illustrate the relationship between τ_i and $\mathcal{V}_{\alpha=0}^{\text{spec } i}$ in Fig. G1 (inset panels). For the six communities of Fig. 5, we fit the power-law relationship

$$\mathcal{V}_{\alpha=0}^{\text{spec } i} \propto \tau_i^{\nu}, \tag{G3}$$

where the index i runs over the set of persistent species. The estimates of the exponent ν (using linear regression on the log-log plot) are all close to one. This result is obvious for the communities without interactions, for which $\mathcal{V}_{\alpha=0}^{\text{spec } i} = \frac{1}{2}\tau_i$ ~~(see also Discussion).~~ left-hand panels). But the same result remains valid in the presence of interactions. We find that interactions do not substantially modify the time scale on which a species responds to perturbations affecting only that species.

~~Without interactions, we have $N_0 = K_0$ and therefore $\tau_0 = 1/r_0$. In this case the time scale of that speciesdynamics is set by the inverse of its growth rate, *a priori* unrelated to its abundance K_0. This is the case in the example on the first row~~ %DIF ¿
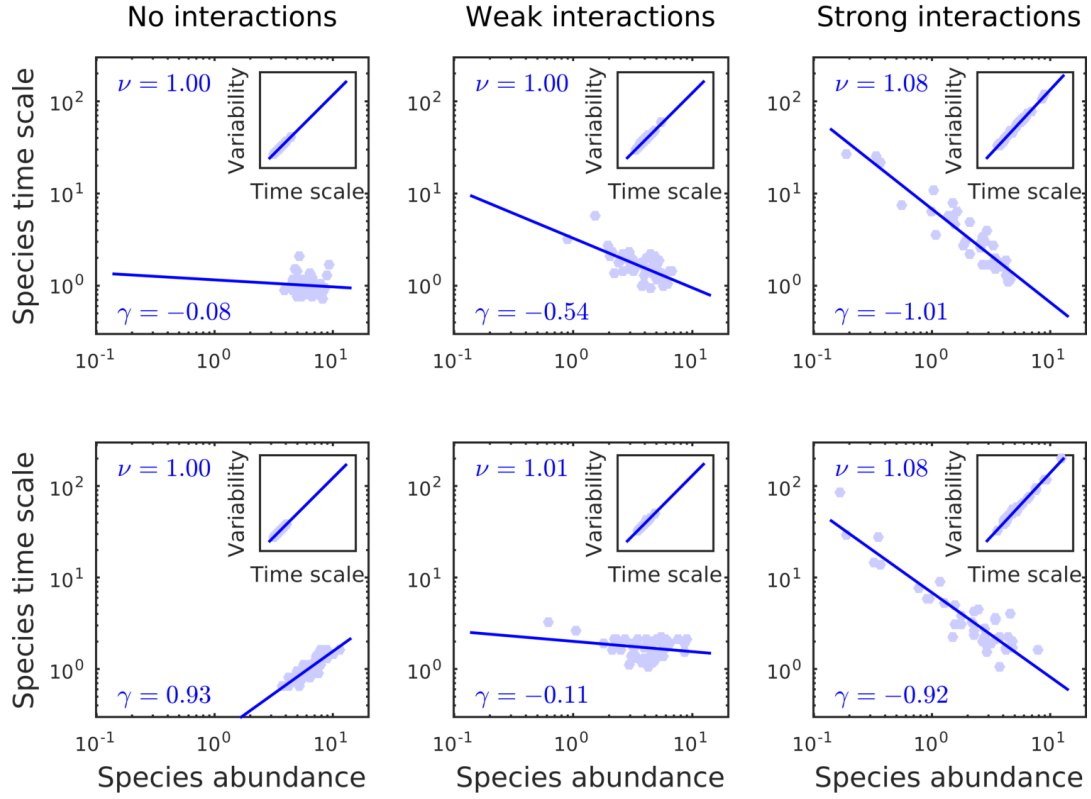
67

Figure G1: Clarifying the relationship between abundance of perturbed species and community variability. In Appendix G we introduce the auxiliary variable τ_i, the characteristic time scale of species i, to explain the relationship between variability $\mathcal{V}_{\alpha=0}^{\mathrm{spec}\ i}$ and abundance N_i. For the six communities of Fig. 5 in the main text, we plot τ_i vs N_i in the main panels, and $\mathcal{V}_{\alpha=0}^{\mathrm{spec}\ i}$ vs τ_i in the inset panels. We fit a power law to each of these relationships, using linear regression on the log-log plot. The estimated exponents γ (for the data τ_i vs N_i) and ν (for the data $\mathcal{V}_{\alpha=0}^{\mathrm{spec}\ i}$ vs τ_i) are reported in the panels.

Therefore, to study the relationship between N_i and $\mathcal{V}_\alpha^{\mathrm{spec}\,i}$, we can restrict to the simpler relationship between N_i and $\tau_i = \frac{K_i}{r_i N_i}$, which is determined by the correlations between growth rates r_i, carrying capacities K_i and equilibrium abundances N_i. Fig. G1 (main panels) shows this relationship for the six communities of Fig. ~~5, in which we drew~~ 5. Fitting the power law

$$\tau_i \propto N_i^\gamma, \tag{G4}$$

we find various estimates for the exponent γ. Without interactions, we have $N_i = K_i$, and hence, $\tau_i = \frac{1}{r_i}$. If growth rates and carrying capacities ~~independently. Alternatively~~ are drawn independently, abundance and response time are unrelated, leading to $\gamma \approx 0$ (Fig. G1, ~~we could assume some trade-off between~~ upper-left panel). Alternatively, if growth rates and carrying capacities ~~, causing low abundance to be associated with lower contribution to variability, illustrated on the second row of~~ satisfy some trade-off, higher abundance (larger K_i) is associated with longer response time (smaller r_i), leading to $\gamma > 0$ (Fig. ~~5. In other words, without interactions, there is no clear relationship to be expected between abundance of perturbed species and variability.~~

~~If species interact, however, the focal species equilibrium abundance will satisfy~~

$$N_0 = K_0 + \sum_j B_{0j} N_j,$$

~~where the sum measures the contribution of all~~ G1, lower-left panel). When increasing the interactions, the link between N_i and K_i becomes weaker. Indeed, from the equilibrium

condition for species i we have

$$N_i = K_i + \sum_{j \neq i} B_{ij} N_j$$

$$= K_i + \left(\sum_{j \neq i} B_{ij} K_j + \sum_{k \neq j \neq i} B_{ij} B_{jk} K_k + \sum_{l \neq k \neq j \neq i} B_{ij} B_{jk} B_{kl} K_l + \dots \right),$$

where in the second line we have used the equilibrium condition for the other species. ~~This term involves potentially very indirect effects between species. Other surviving species satisfy similar conditions so that~~

$$N_0 = K_0 + \sum_j B_{0j} K_j + \sum_{j,k} B_{0j} B_{jk} K_k + \sum_{j,k,l} B_{0j} B_{jk} B_{kl} K_l + \dots$$

~~where we see direct interactions $j \rightsquigarrow 0$ (B_{0j}) but also indirect effects $k \rightsquigarrow j \rightsquigarrow 0$ ($B_{0j} B_{jk}$) and so on. Hence, if the overall interactions with all other species plays a preponderant role in determining the focal species abundance, then the carrying capacity K_0 will not control N_0. Hence, the characteristic time scale τ_0 of the focal species can become inversely proportional to its abundance N_0. If this is the case,~~ For sufficiently strong interactions, the terms between brackets dominate the term K_i, so that N_i and K_i become unrelated. In this case, we have $\tau_i \propto \frac{1}{N_i}$, leading to $\gamma \approx -1$: more abundant species have faster dynamics and ~~generate a smaller response if perturbed independently of their abundance, that is, if the perturbation is of the immigration type ($\alpha = 0$). This explains the~~ smaller response time. This limiting case is observed both if r_i and K_i are independent, and if they satisfy a trade-off (Fig. G1, right-hand panels).

Finally, putting together eqs. (G1, G3, G4), we get

$$\mathcal{V}_\alpha^{\text{spec } i} \propto N_i^\alpha \, \tau_i^\nu \propto N_i^{\alpha+\gamma\nu} \approx N_i^{\alpha+\gamma}, \tag{G5}$$

where in the last step we have used that $\nu \approx 1$. The relationship between abundance ~~and variability shown in the leftmost panel of Fig. 4. If perturbation intensity depends on species abundance~~ of perturbed species and community variability is strongly determined by the exponent γ, that is, by the relationship between abundance N_i and response time τ_i. In the case of weak interactions, the latter relationship depends on the assumed link between growth rate r_i and carrying capacity K_i, so that no unambiguous relationship is to be expected between abundance and variability. However, in the ~~case of demographic-type $(\alpha = 1)$ or environmental-type $(\alpha = 2)$ perturbations, we obtain the relationships shown in the other two panels of Fig. 4. In summary, if species interactions are sufficiently strong and heterogeneous, we expect clear relationships between abundance of perturbed species~~ limit of strong interactions, we have $\gamma \approx -1$ and ~~community variability~~

$$\mathcal{V}_\alpha^{\text{spec } i} \propto N_i^{\alpha-1}. \tag{G6}$$

Hence, for immigration-type perturbations $(\alpha = 0)$ variability is inversely proportional to the abundance of the perturbed species. In contrast, for environmental perturbations $(\alpha = 2)$, variability is directly proportional to the abundance of the perturbed species. These are the relationships depicted in Figs. 4 and 5 of the main text.

H Variability and abundance statistics

From the observed relationship between abundance and variability (Figs. 4 and 5), patterns for worst- and mean-case variability can be deduced. This reveals a connection between stability and diversity metrics.

~~Conisder the variability~~ Denote by $\mathcal{V}_\alpha^{\mathrm{spec}\ i}$ ~~caused by a perturbation of type~~ the community variability induced by a type-α ~~,~~ perturbation fully focused on species i. ~~In communities with strong and heterogeneous interactions~~ (We start from the power-relationship (G6), linking this variability and the equilibrium abundance of species i. As argued in Appendix G~~) we have that~~

$$\mathcal{V}_\alpha^{\mathrm{spec}\ i} \propto \underbrace{N_i^\alpha}_{\mathrm{perturbation}} \times \underbrace{N_i^{-1}}_{\mathrm{response}} = N_i^{\alpha-1}.$$

, we expect this relationship to hold for sufficiently strong interactions.

For immigration-type perturbations ($\alpha = 0$), worst-case variability is approached by taking the maximum over species which gives

$$\mathcal{V}_{\alpha=0}^{\mathrm{worst}} \approx \max_i \mathcal{V}_{\alpha=0}^{\mathrm{spec}\ i} \propto \frac{1}{\min_i N_i}. \tag{H1}$$

so that ~~worst-case variability~~ the worst case is governed by the rarest species. ~~Furthermore,~~ Because the abundance of the rarest species typically decreases with diversity, ~~so that~~ the corresponding diversity-stability relationship is decreasing. For mean-case variability, averaging over species individual contributions, we get

$$\mathcal{V}_{\alpha=0}^{\mathrm{mean}} = \frac{1}{S} \sum_i \mathcal{V}_{\alpha=0}^{\mathrm{spec}\ i} \propto \frac{1}{S} \sum_i \frac{1}{N_i} = \langle N \rangle_{\mathrm{harm}}^{-1}, \tag{H2}$$

where $\langle N \rangle_{\mathrm{harm}}$ stands for the harmonic mean of species abundances. Mean abundance typ-

ically decreases with diversity, so that the corresponding diversity-stability relationship is decreasing.

When caused by environmental-type perturbations ($\alpha = 2$), ~~variability is proportional to the abundance of the perturbed species, so that the worst case is~~ worst-case variability is approached by taking the maximum over species, giving

$$\mathcal{V}_{\alpha=2}^{\mathrm{worst}} \approx \max_i \mathcal{V}_{\alpha=0}^{\mathrm{spec}\ i} \propto \max_i N_{i\underline{.}}, \tag{H3}$$

so that ~~worst-case invariability~~ the worst case is governed by the most abundant species. For mean-case variability ~~, averaging over species individual contributions,~~ we get

$$\mathcal{V}_{\alpha=2}^{\mathrm{mean}} \propto \frac{1}{S} \sum_i N_i = \langle N \rangle_{\mathrm{arith}}, \tag{H4}$$

the arithmetic mean of species abundances. Mean abundance typically decreases with diversity, so that the corresponding diversity-stability relationship is increasing.

Note ~~,~~ that when caused by demographic-type perturbations ($\alpha = 1$) the species-by-species approach does not work: demographic variability probes a ~~purely~~ collective property of the community. The different relationships between abundance and variability are illustrated in Fig. H1.

I ~~Population- and ecosystem-level stability~~

~~In this appendix we revisit the diversity-stability relationships reported in Fig. 6. Instead of using average variance, eq. (2), to define variability, as we did so far, let us consider two measures that have been proposed to quantify stability at the ecosystem and at the population level. The first one, $\mathcal{I}^{\mathrm{eco}}$, is simply the inverse CV of total biomass N_{tot}. The second, $\mathcal{I}^{\mathrm{pop}}$, is~~
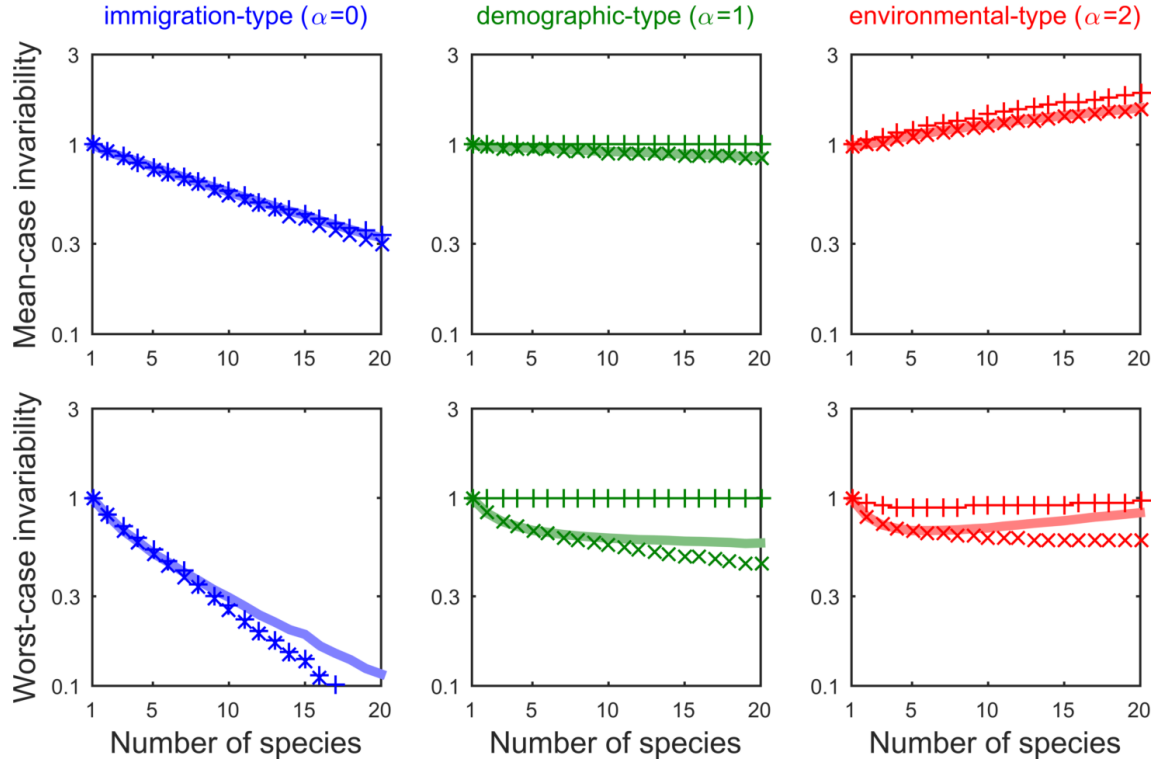
Figure H1: Invariability and species abundance. Top row: mean-case, bottom row: worst-case. ×-marks: analytical formula; +-marks: approximation in terms of abundance (see Appendix H); thick line: simulation results. For immigration-type perturbations (first column, in blue), mean-case invariability scales as the harmonic mean abundance (see eq. (H2)), which decreases with diversity. Worst-case invariability scales as the abundance of the rarest species. On the other hand, in response to environmental-type perturbations (third column, in red), mean-case variability scales as the arithmetic mean abundance (see eq. (H4)) so that invariability increases. Worst-case variability scales as the abundance of the most common species. In between (second column, in green), for demographic-type perturbations, neither worst- nor mean-case invariability is determined by statistics of species abundances.

the inverse weighted mean CV of species biomass. More precisely if $p_i = N_i/N_{tot}$, we define

$$\mathcal{I}^{\text{eco}} = \frac{1}{\text{CV}^2(N_{tot})}; \;\; \mathcal{I}^{\text{pop}} = \frac{1}{(\sum_i p_i \text{CV}(N_i))^2}.$$

On the top row of Fig. I1 we see that $\mathcal{I}^{\text{eco}}$ increases with diversity for all perturbation types. On the bottom row we see that $\mathcal{I}^{\text{pop}}$ decreases with diversity for all perturbation types.

By construction, regardless of perturbation type, $\mathcal{I}^{\text{eco}}$ gives a predominant weight to abundant species while also allowing for buffering effects driven by synchrony between species time-series (Loreau and de Mazancourt, 2013). On the other hand, regardless of perturbation type, $\mathcal{I}^{\text{pop}}$ gives a large weight to rare species.

In fact, along any environmental gradient $\mathcal{I}^{\text{pop}}$ detects transcritical bifurcations, i.e. goes to zero whenever a species gradually becomes extinct (Haegeman and Loreau, 2011). In this sense it is clearly sensitive to the presence of rare species. On the other hand, $\mathcal{I}^{\text{eco}}$ relates to the variability of total biomass which, by construction gives more weight to abundant species than to rare ones, but is also known to be a very specific direction in phase-space. Indeed, for competitive systems, due to species compensation, it is the most stable directions, i.e. the direction along which perturbations are absorbed the fastest (Allesina and Tang, 2012; Arnoldi et al., 2016) . This effect was not present in the measure used in the main text, i.e. average variance, seen as the outcome of a random sampling over directions of observations (see Appendix B).

We see here the strong effect that the choice of observation can have on variability patterns, due to emphasis it puts on specific species abundance classes.